Check for updates

View Article Online
View Journal

Energy & Environmental Science

Accepted Manuscript

This article can be cited before page numbers have been issued, to do this please use: Y. Ren, C. Yu, X. Tan, H. Huang, Q. Wei and J. Qiu, *Energy Environ. Sci.*, 2021, DOI: 10.1039/D0EE03596C.

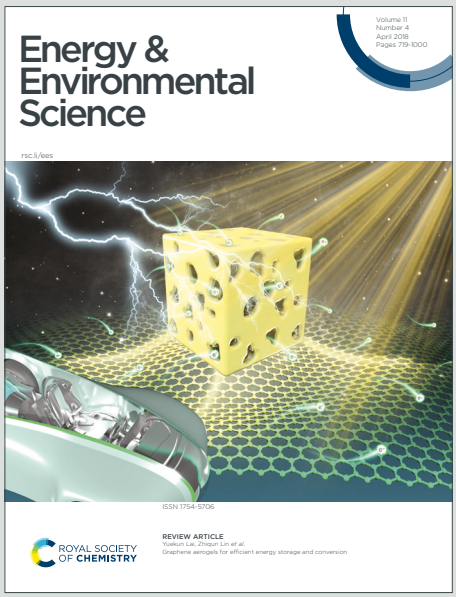

This is an Accepted Manuscript, which has been through the Royal Society of Chemistry peer review process and has been accepted for publication.

Accepted Manuscripts are published online shortly after acceptance, before technical editing, formatting and proof reading. Using this free service, authors can make their results available to the community, in citable form, before we publish the edited article. We will replace this Accepted Manuscript with the edited and formatted Advance Article as soon as it is available.

You can find more information about Accepted Manuscripts in the Information for Authors.

Please note that technical editing may introduce minor changes to the text and/or graphics, which may alter content. The journal's standard Terms & Conditions and the Ethical guidelines still apply. In no event shall the Royal Society of Chemistry be held responsible for any errors or omissions in this Accepted Manuscript or any consequences arising from the use of any information it contains.

ROYAL SOCIETY OF CHEMISTRY

rsc.li/ees

View Article Online
DOI: 10.1039/D0EE03596C

Published on 19 January 2021. Downloaded by Dalian University of Technology on 1/24/2021 11:50:40 AM.

ARTICLE

Strategies to Suppress Hydrogen Evolution for Highly Selective Electrocatalytic Nitrogen Reduction: Challenges and Perspectives

Received 00th January 20xx,
Accepted 00th January 20xx

DOI: 10.1039/x0xx00000x

Yongwen Ren,[a] Chang Yu,*[a] Xinyi Tan,[a] Hongling Huang,[a] Qianbing Wei[a] and Jieshan Qiu*[ab]

Ammonia, as a significant chemical for fertilizer production and also a promising energy carrier, is mainly produced through the traditional energy-intensive Haber−Bosch process. Recently, electrocatalytic N_2 reduction reaction (NRR) for ammonia synthesis has received tremendous attention with the merits of energy saving and environmental friendliness. To date, the development of NRR process is primarily hindered by the competing hydrogen evolution reaction (HER), whereas the corresponding strategies for inhibiting this undesired side reaction to achieve high NRR selectivity are still quite limited. Furthermore, for such a complex reaction involving gas-liquid-solid three phases and proton/electron transferring, it is also rather meaningful to decouple and summarize the current strategies for suppressing the H_2 evolution in terms of NRR mechanisms, kinetics, thermodynamics, and electrocatalyst design in detail. Herein, on the basis of the NRR mechanisms, we systematically summarize the recent strategies to inhibit the HER for highly selective electrocatalytic NRR, focusing on limiting the proton- and electron-transfer kinetics, shifting the chemical equilibrium, and designing the electrocatalysts. Additionally, the insights into boosting the NRR selectivity and efficiency for practical applications are also presented in detail with regard to the determination of ammonia, the activation towards N_2 molecule, the regulation of gas-liquid-solid three-phase interface, the coupled NRR with value-added oxidation reactions, and the development of flow cell reactor.

1. Introduction

The Ammonia (NH_3) is one of the most significant chemicals as it plays a vital role in the chemical and hydrogen storage industries.[1,2] The industrial production of NH_3 heavily depends on the conventional Haber−Bosch process under relatively harsh conditions such as high temperatures (400–600 °C) and pressures (20–40 MPa).[3,4] Moreover, this process accounts for more than 1% of the global annual energy consumption and generates ~300 metric tons of CO_2 per year.[3,5,6] Therefore, a sustainable and scalable synthetic route for NH_3 is highly required. Electrocatalytic N_2 reduction reaction (NRR) to NH_3, aiming to replace the energy-intensive Haber−Bosch process, not only conducts at ambient conditions but also can be driven by the renewable intermittent energy including solar energy, wind energy, etc.[3,7–9] In fact, since the pioneering work was reported in the later 1960s, such an approach has been explored for a long time and fast developed recently.[8,10] For example, the corresponding NRR Faradaic efficiency (FE) changed and increased accompanied by the developed electrocatalysts for this system, which was summarized in Fig. 1. In 1969, van Tamelen et al. successfully developed an electrocatalytic NRR system using Ti (Ⅱ) as the active species.[11] Afterwards, in 1971–2015, the development of the NRR work kept relatively slow, where only less work focused on this aspect. Specifically, in 1998, Marnellos and Stoukides employed Pd as the catalyst and achieved a NRR FE of ~1%.[7] In 2000, Kordali et al. reported a solid polymer electrolyte cell with a Ru particle at atmospheric pressure and low temperature, yielding a NRR FE of 0.92%.[12] In summary, these early attempts not only successfully designed and operated the NRR device, of course, including the catalysts and electrolytes in this system, but also had confirmed that the low FE for NH_3 production (generally less than 1%) was primarily caused by the competing hydrogen evolution reaction (HER). In the following years, in order to further improve the NRR FE, extensive studies had been carried out in terms of catalyst screening and reaction configuration optimization, and the FEs of 2–10% for NH_3 production were obtained. Meanwhile, a series of catalysts for NH_3 synthesis were developed such as the noble metal-containing electrocatalysts (Pd, Au, Ru, etc.), non-noble metal-based electrocatalysts (Mo, Fe, Ti, Co, Ni, etc.) and metal-free electrocatalysts (B-doped graphene, black phosphorus, etc.).[13–21]

Since 2019, more and more efforts have been devoted to building the efficient methods for precise ammonia detection and at the same time, the FE for NH_3 synthesis is further improved in a range of 10–20%.[8,10,22,23] However, such a NRR FE is still relatively low and is far below that required for NH_3 synthesis implementation at scale mainly because of the severely competitive HER process, and the detailed reasons can be summarized as the following aspects. It is well known that the NRR process in aqueous media involves multiphase-reactions and complex transfer schemes, including six protons

[a] State Key Laboratory of Fine Chemicals, Liaoning Key Lab for Energy Materials and Chemical Engineering, School of Chemical Engineering, Dalian University of Technology, Dalian 116024, China. E-mail: chang.yu@dlut.edu.cn; jqiu@dlut.edu.cn
[b] State Key Laboratory of Chemical Resource Engineering, College of Chemical Engineering, Beijing University of Chemical Technology, Beijing 100029, China. E-mail: qiujs@mail.buct.edu.cn

Energy & Environmental Science Accepted Manuscript

View Article Online
DOI: 10.1039/D0EE03596C

Published on 19 January 2021. Downloaded by Dalian University of Technology on 1/24/2021 11:50:40 AM.

and a N_2 molecule from the electrolyte as well as six electrons derived from the external circuit.[4] By comparison, the HER process is much faster, which only needs two protons and two electrons.[24,25] Besides, it is revealed that most of catalytic materials are intrinsically in favor of the adsorption of H atom over N_2 molecule, finally leading to the fact that a majority of surface active sites and electrons are occupied by the undesired hydrogen (H) atom and then the poor selectivity is delivered.[26] From the thermodynamic perspective, although the similar theoretical potentials are required by both NRR and HER, the NRR actually proceeds at a large overpotential due to the high activation energy barrier of strong N≡N triple bond with a bond energy of 940.95 kJ mol^{-1}.[27] As a result, within the applied potential window where the NRR occurs, the undesirable HER process is usually dominant. Specifically, as presented in the inset of Fig. 1, most of the NRR catalysts generally operate in the low potential window (0.1 to –0.5 V versus reversible hydrogen electrode (*vs.* RHE)), and accordingly, a small current density is obtained for the purpose of maintaining a reasonable selectivity. Furthermore, once the applied reduction potential progressively becomes more negative to produce a large current density, the NRR FEs dramatically reduces due to the detrimental H_2 evolution. Therefore, if the HER process can be effectively suppressed, the bottleneck problems of NRR that are the low selectivity and conversion efficiency can be greatly alleviated and even resolved, which will also promote the practical application of NRR process.

In fact, for such a cutting-edge field, a mass of papers (more than 1,000 papers) have been published in past decade, where the papers mainly focus on the development of catalyst and account for 90.7% (Fig. 2a). With the deep recognition and understanding of this process for quickly facilitating the development of NRR technique, the HER suppression over NRR that is extremely significant/bottlenecked issue, is gradually concerned to improve the selectivity of target product NH_3. Recently, the related work begins to fast present, where ~10% of the papers involve the HER suppression. These papers can be easily classified according to kinetic regulation, thermodynamic regulation, and catalyst design, which are summarized in Fig. 2b. As such, it is highly demanded to summarize the strategies for inhibiting the undesired HER in terms of NRR mechanisms, kinetics, thermodynamics, and design/fabrication of electrocatalysts.

In this review, we discuss recent advances in mechanisms, kinetics, thermodynamics, electrocatalysts, reactor design, as well as process coupling and optimization of the NRR, with a focus on strategies and sought-after routes toward suppressing the H_2 evolution and improving the NH_3 selectivity as the core, to provide constructive guidance toward kinetic regulation, thermodynamic regulation, and electrocatalyst design for scalable and economically feasible applications (Fig. 3). Firstly, we introduce the approaches for suppressing the HER by limiting the proton- and electron-transfer kinetics on the basis of NRR mechanisms. Secondly, from the thermodynamic standpoint, the strategies for mitigating the HER via shifting its chemical equilibrium are presented. Thirdly, we review the representative design strategies for NRR electrocatalyst to inhibit H_2 evolution. Finally, we briefly summarize the remaining challenges in electrochemical NRR field and provide some insights into boosting the selectivity and conversion efficiency from N_2 to NH_3.

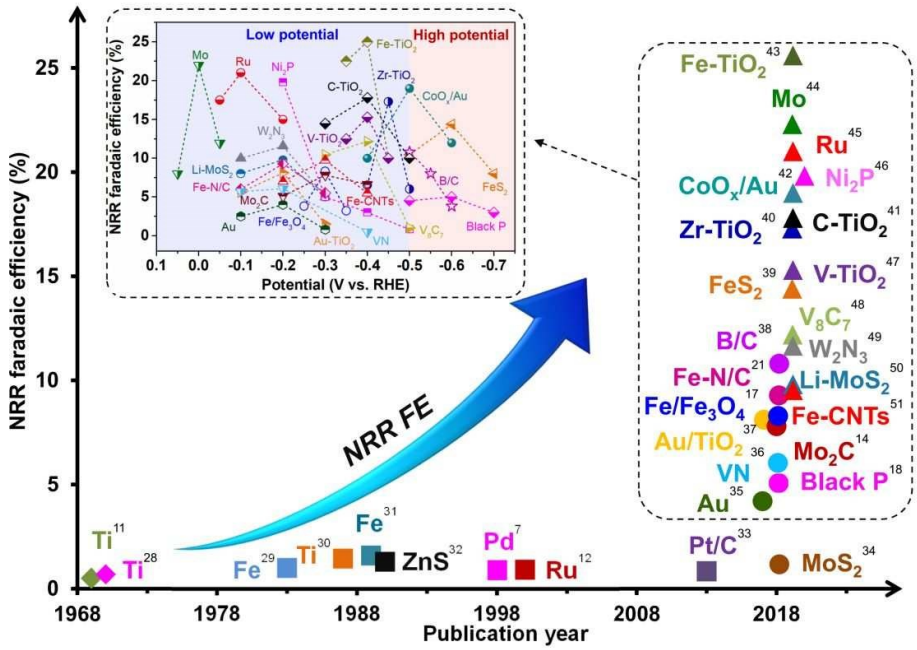

Fig. 1 The road map for the development of used catalysts for NRR process, where the NRR FEs of different catalysts are plotted against the publication year scale. The inset is the variations of NRR FEs over different catalysts *vs.* the applied potentials.

This journal is © The Royal Society of Chemistry 20xx

Please do not adjust margins

Energy & Environmental Science Accepted Manuscript

View Article Online
DOI: 10.1039/D0EE03596C
Journal Name ARTICLE

Published on 19 January 2021. Downloaded by Dalian University of Technology on 1/24/2021 11:50:40 AM.

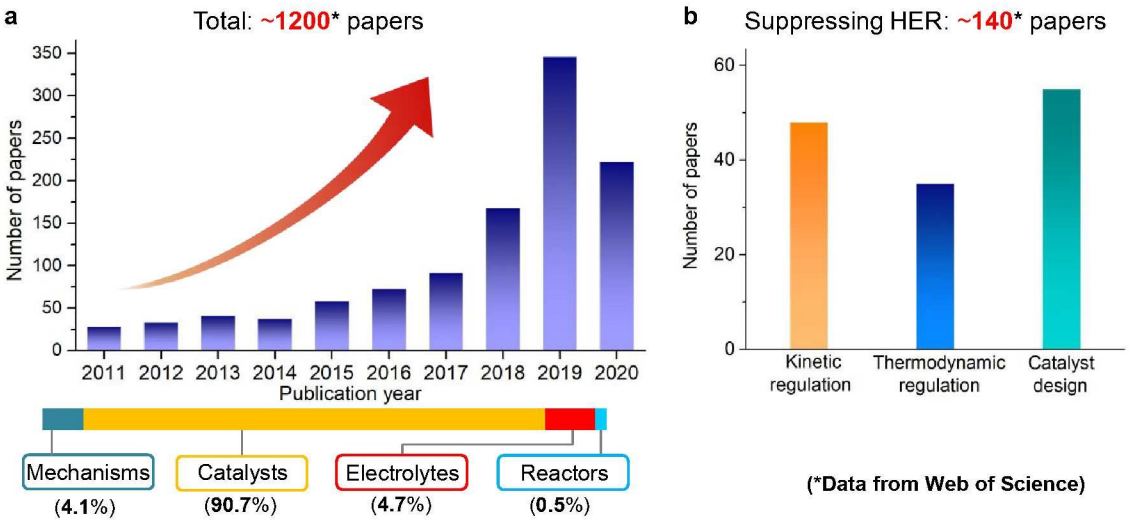

Fig. 2 (a) Histogram of number of papers against the publication year in NRR field. The bar below the histogram denotes the percentages of papers classified by mechanisms, catalysts, electrolytes, and reactors. (b) Histogram of number of publication papers covering HER suppression strategies to boost NRR selectivity, where the papers are classified by kinetic regulation, thermodynamic regulation, and catalyst design.

2. NRR mechanisms

In general, the reaction mechanisms for electrocatalytic NRR process on the surface of heterogeneous catalysts can be divided into dissociative and associative mechanisms (Fig. 4a).[52–54] For the dissociative mechanism, the N≡N triple bond is first cleaved, and the hydrogenation steps subsequently take place over the adsorbed N atoms. It should be noted that such a mechanism is uncommon in the NH_3 electrosynthesis under ambient conditions due to a rather high energy required by the cleavage of N≡N bond. In the case of associative mechanism, the N_2 molecule is first adsorbed on the surface of catalyst, and then the hydrogenation steps occur over the two N atoms through distal or alternating pathways. As for the distal pathway, the N atom away from the catalyst surface preferentially and continuously obtains H atom from proton

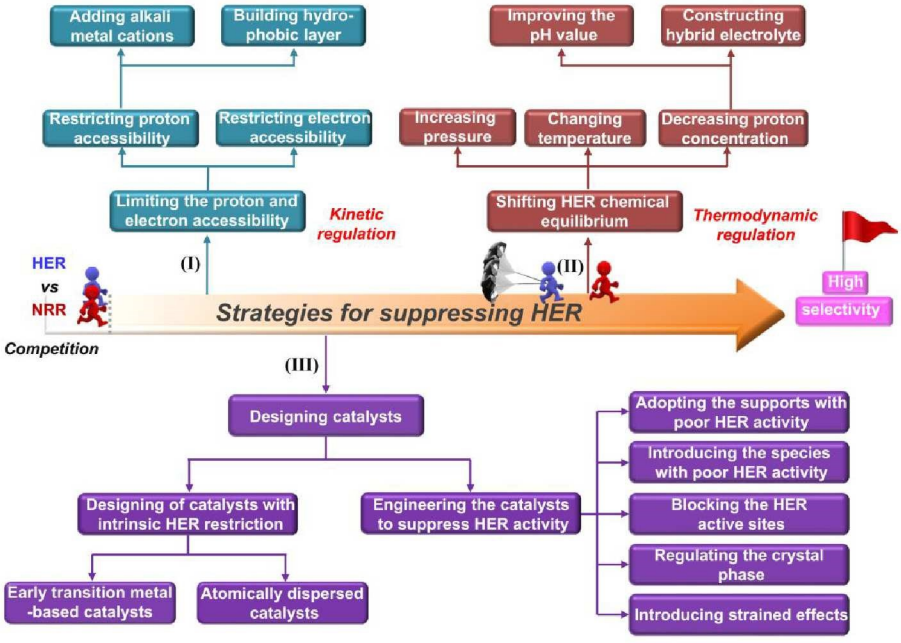

Fig. 3 Strategies to suppress the competing HER for highly selective electrochemical N_2 reduction to NH_3, including limiting the proton and electron accessibility, shifting HER chemical equilibrium, and designing catalysts. The blue cartoon character equipped with a deceleration parachute represents the suppression for HER.

Energy & Environmental Science Accepted Manuscript

Please do not adjust margins

View Article Online
DOI: 10.1039/D0EE03596C

Published on 19 January 2021. Downloaded by Dalian University of Technology on 1/24/2021 11:50:40 AM.

donor of the electrolyte until the complete formation of a NH_3 molecule, and then the remained N atoms on the catalyst surface start to accept H atom to create another NH_3 molecule. While in the alternating pathway, the two N atoms of the N_2 molecule adsorbed through an end-on mode alternately undergo the hydrogenation process until a NH_3 molecule is released and the N−N bond is broken. It should be pointed out that the alternating or distal pathways greatly depend on the electrocatalysts in the real NRR process at present. If the N_2 molecule is adsorbed through a side-on mode and undergoes the hydrogenation in the alternating pathway (Fig. 4b), such a different pathway is named as enzyme catalysis that is infrequent in heterogeneous catalysis.[55–57] Especially, for the transition metal nitrides (TMNs), Abghoui and Skúlason revealed that the Mars-van Krevelen (MvK) mechanism was more favorable than both the typical dissociative and associative mechanisms toward electrochemical NH_3 synthesis.[36,58–61] As depicted in Fig. 4c, in the MvK mechanism for NRR, the lattice N atoms in TMNs surface are reduced to NH_3 molecules; meanwhile, abundant N vacancies are generated on the surface. Subsequently, these N vacancies are filled continuously by the gaseous N_2 to maintain the NRR process.

The mechanisms of electrochemical NRR are still under elusive, and the mechanisms are usually different over various catalysts.[62] According to the general mechanism, the electrocatalytic NRR process basically involves four steps: N_2 adsorption on the catalyst surface, N≡N bond activation by either proton transfer from proton donor or electron injection from external circuit, the continuous proton-coupled electron transfer (PCET) steps, and the formation of NH_3 molecule.[5,63,64] In contrast to the PCET steps, the adsorption and activation for N_2 molecules are relatively easy and fast over most of NRR catalysts.[53,65] More precisely, the first hydrogenation procedure of adsorbed N_2 molecule ($*N_2 + H^+ + e^- \rightarrow *N_2H$) in the PCET process has been commonly regarded as the rate-determining step (RDS) in NRR process, where "*" denotes the active sites over the surface of catalyst.[65,66] In comparison, the HER also involves the PCET steps, yet it is much faster in kinetics via the Volmer−Heyrovsky or Volmer−Tafel mechanisms, which finally results in a relatively low NRR selectivity.[1,5,67]

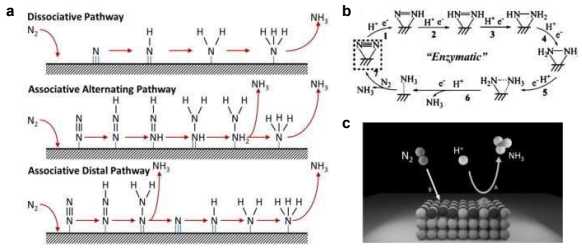

Fig. 4 The reaction mechanisms for electrocatalytic NRR process. (a) Dissociative pathway, associative distal and alternating pathways. Reproduced with permission from ref.[52]. Copyright 2017, Elsevier. (b) Enzymatic pathway. Reproduced with permission from ref.[54]. Copyright 2018, Wiley-VCH. (c) Mars-van Krevelen pathway. Reproduced with permission from ref.[61]. Copyright 2019, Springer.

3. Limiting the proton and electron accessibility—kinetic regulation

As discussed above, both NRR and HER processes involve the transfer of proton and electron, and the HER is much faster than the NRR in kinetics. With this in mind, to mitigate the competing H_2 evolution, the proton- and electron-transfer kinetics in electrocatalytic NRR process deserve to be rationally regulated. It has been confirmed by Nørskov and co-workers that the production rate of NH_3 is not correlated with the proton and electron concentrations; on the contrary, the production rate of H_2 is dependent on both the proton and electron concentrations in first-order relevance.[66] That is to say, limiting the accessibility of proton and electron can effectively inhibit the kinetically preferred HER process, while do not affect the NH_3 synthesis process. Accordingly, on the basis of the mechanisms, the strategies for suppressing HER process can be presented in view of kinetics as following: limiting the accessibility of proton and electron during NRR process. With these two processes being well controlled, the applied potential for NRR can be lowered to be more negative, and at the same time, the conversion efficiency will be greatly enhanced.[5,53,66,68]

3.1. Limiting the proton accessibility

It is well known that there exists an electrical double layer (EDL) at the interface between electrolyte and catalyst, where the behaviors of ions and molecules are remarkably different from the bulk solution (Fig. 5).[69] Furthermore, it is highlighted that the structure of EDL is of great significance for the activity and selectivity of electrocatalytic reaction.[70] In the case of NRR process, it has been pointed out that reducing the transfer rate of proton donor can limit its accessibility in kinetics, finally leading to a suppressed H_2 evolution and a boosted NRR selectivity.[66] Therefore, it is highly desired to decrease the transfer rate of proton donor in the electrolyte, especially in the EDL. Current strategies can be mainly considered and built in terms of electrolytes and electrocatalysts, including adding the alkali metal cations into electrolytes and building hydrophobic protection layer on the surface of electrocatalysts, respectively.

3.1.1. Adding the alkali metal cations into electrolytes. On the one hand, the transfer rate of proton donor can be effectively reduced by adding the alkali metal ions (such as Li^+, Na^+, and K^+ ions, etc.) due to the solvation and steric effects (Fig. 5a).[19,71–73] For instance, Rondinone and co-workers investigated the effects of Li^+, Na^+, and K^+ ions in electrolyte on the NRR FE over N-doped carbon nanospike (CNS) catalyst, respectively.[74] It was found that under the differently applied potentials including −0.8, −1.0, and −1.2 V (*vs.* RHE), the highest NRR FE of CNS was all observed in the Li^+-contained electrolyte, and the FE significantly dropped as the size of alkali metal ion increased ($Li^+ < Na^+ < K^+$). To confirm this, the corresponding mechanism was also decoupled via theoretical simulation. The results showed that the smallest Li^+ ion was more favorable for forming a dehydrated cation layer on the surface of CNS due to the strong solvent effects, thereby increasing the transfer barrier of H_2O molecules and impeding the HER in water splitting. Likewise, Yan et al. also found that a solvation layer related to the K^+ ion in electrolyte was constructed on the surface of bismuth

Energy & Environmental Science Accepted Manuscript

This journal is © The Royal Society of Chemistry 20xx

Please do not adjust margins

View Article Online
DOI: 10.1039/D0EE03596C

Published on 19 January 2021. Downloaded by Dalian University of Technology on 1/24/2021 11:50:40 AM.

nanocrystal (BiNC) catalyst, and the solvation layer could significantly retard the migration of proton donor in the EDL.[75] Additionally, as the concentration of K^+ ion increased from 0.2 to 1.0 mol L^{-1}, the delivered current density for the BiNC catalyst raised from 0.14 to 0.50 mA cm^{-2} for NRR but that reduced from 1.31 to 0.25 mA cm^{-2} for HER. The resultant NRR FE was also promoted from 9.8 to 67%. Similar inhibition effects for HER induced by Li^+, Na^+, and K^+ ions in the electrolytes were also presented for Au-, Ag-, Pt-, and Fe-based catalysts.[75–77] In conclusion, because of the solvation and steric effects, the alkali metal ions can remarkably slow the transfer rate of H_2O molecule (proton donor) in the EDL indeed, which can suppress the HER activity and is not restricted by the adopted catalysts. In addition to this, these alkali metal ions (especially the K^+ ions) were also able to promote the adsorption of N_2 molecules on the surface of catalyst.[78] Furthermore, in the non-aqueous electrolytes, the Li^+ ions also play a prominent part in mediating the reaction pathways of NRR through the reaction of produced Li metal and N_2 molecule.[79,80] Due to the greatly limited proton accessibility in the non-aqueous electrolytes, the Li-mediated NRR process usually can achieve a high selectivity of NH_3 compared with aqueous NRR. However, it was pointed out that the commercial lithium salts, such as Li_2CO_3, Li_2SO_4, and $LiClO_4$ all contained inevitable trace amount of NO_3^- and NO_2^-, resulting in a false positive result for electrochemical NRR, thus this strategy should be adopted with more cautions.[81] In another case, Botte et al. reported that the gel electrolyte of polyacrylic acid homopolymer also helped to decelerate the transport of water, thereby impeding the competing HER side reaction and boosting the NRR FEs over Pt and Ir nanoparticles.[82]

3.1.2. Building hydrophobic protection layer on catalyst surface. On the other hand, building a hydrophobic protection layer on the surface of catalyst via the surface engineering can also effectively slow the transport rate of H_2O (proton donor) owing to the hydrophobic effects (Fig. 5b).[10,54,83,84] For example, Ling et al. coated a hydrophobic layer of zeolitic imidazolate framework (ZIF) on the surface of Ag-Au catalyst to suppress the HER activity of the catalyst.[85] Assisted by the ZIF layer, the Ag-Au catalyst exhibited about 4-fold improvement for the NRR FE. Further studies demonstrated that the hydrophobic coating could efficiently repel the accessibility of H_2O molecules to the catalyst, finally leading to an impeded H_2 evolution. Afterwards, to prevent the possible H_2O transport through the pores of ZIF layer, the authors further modified the external surface of ZIF layer with hydrophobic oleylamine molecules.[86] Correspondingly, the competing HER process was further inhibited. Likewise, Wang and co-workers designed a heterostructured catalyst for electrochemical N_2 fixation, where the catalyst was composed of highly dispersed Au nanoparticles (active species) and porous poly(tetrafluoroethylene) (PTFE) framework (hydrophobic layer).[87] It was found that the PTFE-modified Au catalyst presented a considerably increased NRR FE in contrast to the original Au nanoparticle. It was reasoned that the hydrophobic PTFE effectively suppressed the H_2O transport to the surface of Au nanoparticle, thereby hindering the undesired H_2 generation. Meanwhile, it was observed that the PTFE coating permitted the N_2 diffusion and facilitated to form a high N_2 concentration layer on the surface of Au nanoparticle, which was also helpful for the conversion of N_2 to NH_3. More recently, Liu et al. reported a unique "sandwich"-structured catalyst for electrochemical NH_3 synthesis, where the interlayer of catalyst was the active species of Se vacancy-rich $ReSe_2$ and the two sides of that were the hydrophobic carbon fiber.[88] It was demonstrated that the external hydrophobic carbon layer can effectively protect the $ReSe_2$ electrocatalyst from the coverage of H_2O molecules, finally leading to an inhibited H_2 evolution process and a boosted NRR selectivity. In fact, the

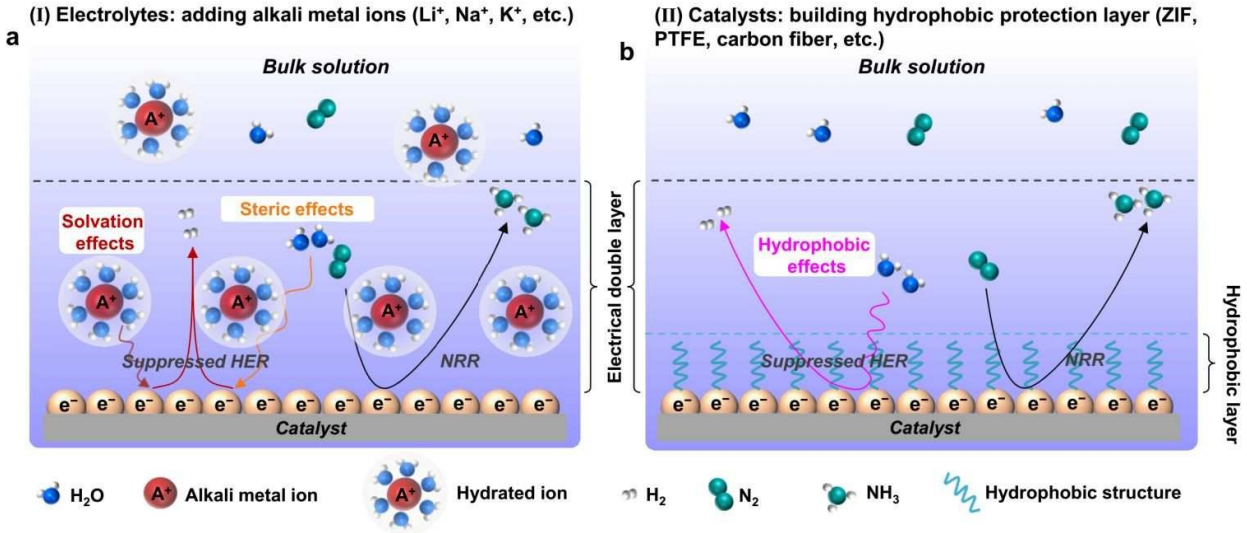

Fig. 5 Strategies for limiting the accessibility of proton donor by adding the alkali metal ions into the electrolyte due to the solvent and steric effects (a), and building hydrophobic protection layer on the surface of catalyst due to the hydrophobic effects (b).

Energy & Environmental Science Accepted Manuscript

Please do not adjust margins

View Article Online
DOI: 10.1039/D0EE03596C

Published on 19 January 2021. Downloaded by Dalian University of Technology on 1/24/2021 11:50:40 AM.

surface engineering strategies for catalysts to restrict the HER process have been generally adopted in other fields, such as the introduced linear alkanethiols in rechargeable iron battery,[89] the incorporated hybrid bilayer membrane in oxygen reduction reaction,[90] and the utilized fluorine interlayer or nitrogen-carbon layer in CO_2 reduction reaction, etc.[91,92] As such, these methods would be also employed to guide the design of NRR catalysts for the purpose of boosting NRR selectivity. Moreover, it should be noted that the strategies including adding alkali metal ions into the electrolyte and building the hydrophobic protection layer on the surface of catalyst mainly focus on the restriction of H_2O transport. While in the acidic media, the proton donor participated in NRR process is in the form of H_3O^+, thus the studies associated with reducing the transport rate of H_3O^+ are also highly required in future.

3.2. Limiting the electron accessibility

As mentioned in Section 2, the HER and NRR processes involve the PCET steps. It was also presented by Nørskov et al. that the difference for them is that the HER is first-order relevance in electron concentration, whereas the NRR is not correlated with the electron concentration.[66] Therefore, the strategy of limiting the accessibility of electron can also effectively suppress the competing H_2 evolution and the NRR process does not be affected. At the present, the electron accessibility during NRR process can be controlled to a great degree via constructing the multilevel configurations in catalyst such as support–semimetal catalyst, the support–conductive polymer catalyst, and support–insulator–catalyst. Specifically, due to the intrinsically sluggish electron accessibility, the semimetals (such as Sn and Bi) can be utilized to build a support–semimetal catalyst configuration, where the electron transfer from the support to the surface of catalyst can be limited (Fig. 6a).[93–96] For example, Qiao et al. constructed a 2D mosaic Bi nanosheets for electrochemical NRR and it was found that the Bi nanosheets featured a relatively large charge-transfer resistance of ~300 Ω, indicative of an effective restriction for electron transfer.[97] As a result, the competing HER was obviously retarded and a high NRR FE of 10.46% was delivered by the Bi nanosheets at a potential of –0.8 V (*vs.* RHE). Likewise, the Sn-based catalysts can also effectively limit the electron transfer during NRR process, thereby suppressing the undesired H_2 evolution. On the basis of this, the applied potentials of the Sn-based catalysts for NRR can be extended to a more negative range, which is helpful to improve the conversion efficiency. Meanwhile, their optimal NRR FEs were also achieved at relatively negative potentials, for example, −0.8 V for Sn/SnS_2 nanosheet, −0.4 V for SnO_2 nanofiber, −0.5 V for SnO_2 quantum dots, −0.8 V for SnO_2 particle, and −0.5 V for SnS_2 nanoarray.[98–102] Furthermore, the theoretical calculations revealed that these semimetals exhibited the rather weak binding ability for H atoms, which also contributed to boosting the NRR selectivity.[103,104] In another case, Röpke et al. selected the conductive polyaniline (PAN) and fabricated a support–PAN electrode for electrocatalytic N_2 fixation, where the PAN coating enabled the NRR process and regulated the electron accessibility (Fig. 6b).[105] Since the thickness of PAN film was highly steerable, the electron transfer rate during NRR process could be effectively controlled. Moreover, it was confirmed that the PAN could also accelerate the adsorption of N_2 molecules and their intermediates.[106] Similarly, other conductive polymers such as polyimide and polypyrrole were also found to drive the electrochemical N_2 fixation and inhibit the HER process.[107,108] In addition, it has been pointed out that the insulator structure can also slow down the transfer rate of electron flux.[109] Recently, Nørskov et al. put forward a support-insulator-catalyst electrode configuration for electrochemical NRR (Fig. 6c).[66] Owing to the suppressed electron transfer within the insulator layer, the total transfer rate of electron from support to catalyst could be significantly slowed. It is noteworthy that, although a relatively high NRR selectivity can be delivered via slowing the transfer rate of electron, but the excessive restriction for electron transfer maybe lead to a relatively low conversion efficiency.[110] As such, this approach should be employed with the consideration of the balance between NRR selectivity and efficiency.

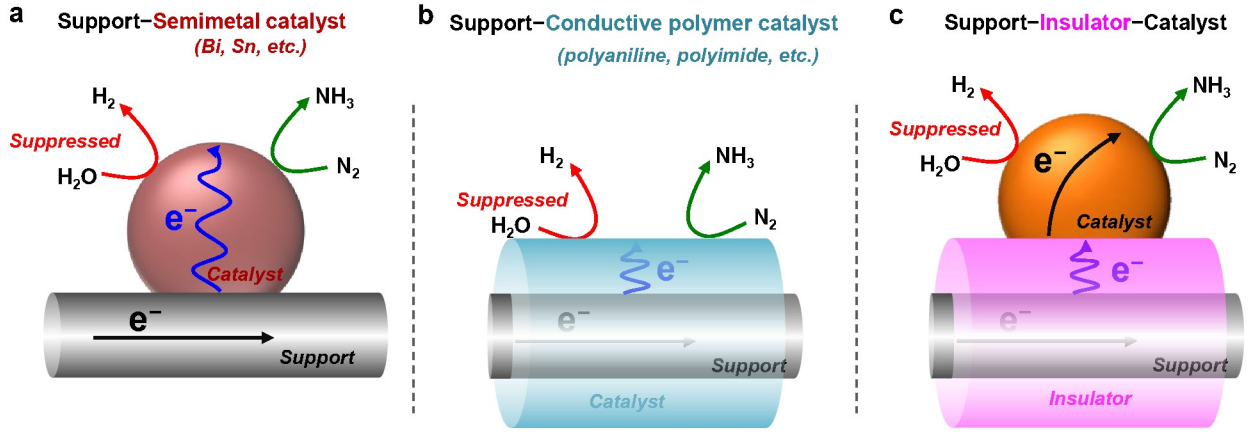

Fig. 6 Strategies for limiting the electron accessibility in NRR process by constructing the multilevel electrode configurations including the support–semimetal catalyst (a), support–conductive polymer catalyst (b), and support–insulator–catalyst (c).

This journal is © The Royal Society of Chemistry 20xx

Please do not adjust margins

Energy & Environmental Science Accepted Manuscript

View Article Online
DOI: 10.1039/D0EE03596C
Journal Name ARTICLE

Published on 19 January 2021. Downloaded by Dalian University of Technology on 1/24/2021 11:50:40 AM.

4. Shifting HER chemical equilibrium—thermodynamic regulation

Above strategies for suppressing the competing HER primarily focused on the proton- and electron-transfer kinetics in the electrocatalytic NRR process. Additionally, from the thermodynamic point of view, the undesirable H_2 evolution can also be effectively inhibited by shifting its chemical equilibrium. The corresponding strategies include increasing the reaction pressure, changing the reaction temperature, and decreasing the concentration of proton donor (Fig. 7).

4.1. Increasing the reaction pressure

It is well known that the electrochemical HER is a typical volume-increased reaction. On the basis of the Le Chatelier's principle, increasing the reaction pressure can shift the chemical equilibrium of HER and suppress its occurrence (Fig. 7a). For instance, Wang and co-workers recently constructed a pressurized reaction system for electrochemical NH_3 synthesis and investigated the influence of reaction pressure on the competing HER in a range of 0.1–0.7 MPa.[111] It was discovered that the competing HER was dominated under ambient pressure condition (0.1 MPa), resulting in a relatively low NRR selectivity. As expected, an increased reaction pressure distinctly inhibited the undesirable H_2 evolution process and improved the NRR FE. Specifically, the as-made Fe_3Mo_3C/C composite nanosheet exhibited a NRR FE of 14.74% at a pressure of 0.7 MPa, approximately 11 times more than that (1.32%) at 0.1 MPa. It is worth noting that the enhancement of reaction pressure can also improve the coverage degree of N_2 molecule on the surface of catalyst due to the significantly increased N_2 solubility in electrolyte (Fig. 7a), which has been proved to be favorable to accelerate the NRR process.[112,113] In this regard, the gas-diffusion electrodes (GDEs) that can increase the local N_2 concentration and overcome the N_2 mass transport issues should be highlighted and used in this system to improve the NRR FE.[114–118] In addition, the pressurized condition can also promote the forward reaction of N_2 electroreduction due to its volume-decreased characteristics. Consequently, appropriate increasing the reaction pressure may be an efficient method to improve the selectivity towards NH_3 and efficiency of NRR electrocatalysts.

4.2. Changing the reaction temperature

According to the Le Chatelier's principle, changing the reaction temperature can also cause the shift in chemical equilibrium. As for the electrochemical HER, a slightly endothermic process ($\Delta H > 0$), reducing the reaction temperature can shift its chemical equilibrium and inhibit the H_2 generation to some degree.[119] Accordingly, the selectivity of NRR will be highly boosted (Fig. 7b). For example, Zou et al. investigated the influence of temperature on NRR selectivity by utilizing CoP hollow nanocages as the electrocatalyst.[16] It was discovered that the NRR FE dramatically reduced as the temperature increased in a range of 25 to 70 °C. The highest FE over the CoP nanocage was observed at 25 °C (4.86%), about three times more than that at

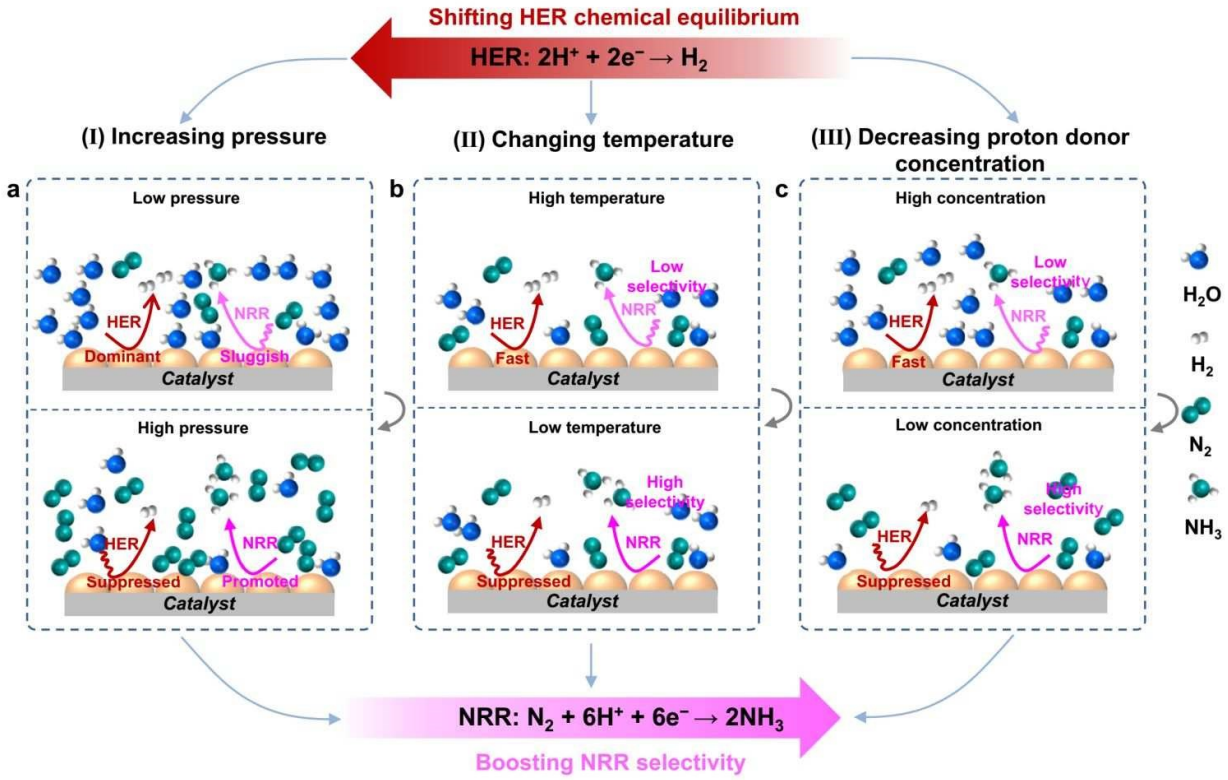

Fig. 7 Strategies for shifting the chemical equilibrium to suppress HER process by increasing reaction pressure (a), changing reaction temperature (b), and decreasing proton donor concentration (c).

Energy & Environmental Science Accepted Manuscript

Please do not adjust margins

View Article Online
DOI: 10.1039/D0EE03596C

Published on 19 January 2021. Downloaded by Dalian University of Technology on 1/24/2021 11:50:40 AM.

70 °C (1.59%). Likewise, Yu and co-workers recently revealed that the selectivity of NRR decreased with the increase of reaction temperature in a range of 25 to 40 °C over a Mo_2C nanodots catalyst.[120] The authors reasoned that the reduced NRR FE arose from the dramatically improved HER process at the higher temperature. Above observations confirm that the reduction of reaction temperature can mitigate the competing H_2 evolution to some degree. At this point, adopting the low reaction temperatures (below the room temperature) may be effective to suppress the competitive HER and enhance the NRR FE, whereas it remains unexplored. Furthermore, it should be pointed out that the excessively low reaction temperature inevitably reduced the conversion efficiency of NRR on the basis of the Arrhenius equation.[10] In addition, some researchers observed that the selectivity of NRR enhanced with the increase of reaction temperature. Therefore, much work needs to be carried out to decouple the potential reasons for the changed chemical equilibrium in future.

4.3. Decreasing the concentration of proton donor

Another crucial parameter that can influence the chemical equilibrium of HER is the concentration of proton donor (H_2O or H_3O^+). Apparently, decreasing the concentration of proton donor can also effectively suppress the competitive HER and improve the NRR selectivity. At present, the corresponding strategies can be classified as improving the pH values of aqueous electrolytes and constructing a low-proton hybrid electrolyte.

4.3.1. Improving the pH value for aqueous electrolyte. As the most prevalent electrolytes in NRR field, the aqueous electrolytes typically include acidic (such as 0.05 M H_2SO_4 and 0.1 M HCl), neutral (such as 0.1 M Na_2SO_4 and 0.1 M phosphate buffer solution (PBS)), and alkaline electrolytes (such as 0.1 M KOH and 0.1 M NaOH).[8,10,121] A distinct difference among these electrolytes is the pH value, which directly determines the concentration of proton donor participated in NRR process and then has a strong impact on the NRR selectivity.[25] For example, Centi and co-workers explored the effects of pH values of electrolytes on the selectivity of NH_3 using a Fe_2O_3-CNT catalyst, specifically, conducting the tests in 0.5 M KOH (pH = 13.7), 0.5 M $KHCO_3$ (pH = 9.4), 0.25 M K_2SO_4 (pH = 7), and 0.25 M $KHSO_4$ (pH = 0.6), respectively.[117] It was observed that the NRR FE of catalyst increased as the increment of pH value, and the highest NRR FE (0.164%) was achieved in 0.5 M KOH, approximately two times more than that in 0.25 M $KHSO_4$ (0.075%). Similarly, taking a nanoporous N-doped carbon catalyst as an example, Wu et al. also revealed that a better NRR selectivity in 0.1 M KOH than that in 0.1 M HCl was presented in an operating temperature range of 25 to 60 °C.[122] Additionally, Cheng et al. observed that the Mo_2C nanodots anchored on carbon cloth catalyst presented a NRR FE of 7.8% in a proton-suppressed electrolyte (pH = 3), while an inferior FE of 1.6% was delivered in a proton-enriched (pH = 2) electrolyte.[14] These observations above indicate that the proton-enriched electrolyte corresponding to low pH value usually leads to an inferior NRR selectivity due to the fast HER process (Fig. 7c). In this regard, employing the neutral PBS electrolyte with intrinsically limited proton availability may be also favorable for impeding the H_2 generation. Recently, Feng and co-workers revealed that a Pd/C catalyst in neutral PBS electrolyte showed the superior NRR selectivity than that in 0.05 M H_2SO_4 and 0.1 M NaOH, due to the restricted H_2 evolution process.[20] This is also the case for a Fe/Fe_3O_4 catalyst.[17] In addition to the pH value of the bulk solution, it was revealed that a high local pH value on catalyst surface can also effectively suppress the HER process.[72]

Another notable aspect is that the pH value of electrolyte also determines the form of proton donor (H_2O or H_3O^+) that participated in NRR process, finally affecting the HER activity and NRR selectivity to some degree (Fig. 8). It is well known that the Volmer step of HER process in neutral or alkaline electrolytes ($H_2O + e^- + * \rightarrow *H + OH^-$) involves the prior water dissociation process that features a high energy barrier, this is not the case for that in acidic medium ($H_3O^+ + e^- + * \rightarrow *H + H_2O$) without water dissociation process.[123,124] Therefore, the HER processes in neutral and alkaline electrolytes are more sluggish in contrast to that in acidic electrolyte due to the restricted Volmer step. Particularly, Strmcnik et al. revealed that most metal catalysts exhibited ~2–3 orders of magnitude lower HER activity in alkaline electrolyte than that in acid medium resulted from the sluggish Volmer step.[125] In this regard, the neutral and alkaline media may be more favorable for achieving a high NRR selectivity compared to acidic solution because of the limited HER activity in neutral and alkaline electrolytes. Nevertheless, it should be noted that the correlation between the pH value of electrolyte and NRR selectivity may be also limited to the cell configurations and catalysts to some degree.[75] To this end, more detailed explorations about the effects of pH values of electrolytes, especially the local pH gradients around the catalyst surface, on the NRR selectivity are highly desired.

4.3.2. Constructing low-proton hybrid electrolyte. Recently, the hybrid electrolyte has been proved to efficiently repress the HER process, of which the water, alcohols, pyridines or amines and aprotogenic (such as dimethyl sulfoxide (DMSO), tetrahydrofuran (THF), and ionic liquids (ILs)) or low-proton solvents (such as alcohols) can be selected as the proton donors and solvents, respectively.[10,30,111,126,127] In such a hybrid electrolyte, the concentration of proton donor can be readily controlled by regulating the ratio of proton donor and solvent, which is favorable for boosting the NRR selectivity as illustrated in Fig. 7c.[66] In 1987, Posin and co-workers investigated the

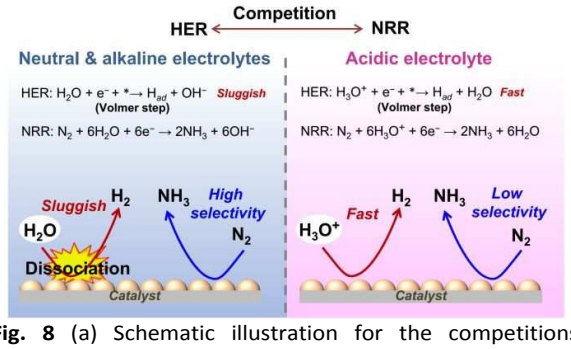

Fig. 8 (a) Schematic illustration for the competitions between HER and NRR in neutral, alkaline, and acidic electrolytes.

Energy & Environmental Science Accepted Manuscript

This journal is © The Royal Society of Chemistry 20xx

Please do not adjust margins

View Article Online
DOI: 10.1039/D0EE03596C

Published on 19 January 2021. Downloaded by Dalian University of Technology on 1/24/2021 11:50:40 AM.

electrocatalytic NRR performance of bis(cyclopentadienyl)titanium (IV) dichloride (Cp_2TiCl_2) catalyst in different hybrid electrolytes of H_2O/THF and H_2O/methanol, respectively.[30] It was found that the catalyst exhibited a higher NRR FE in THF-based electrolyte (0.114%) than that in methanol-based electrolyte (0.017%), indicating that the electrolyte with lower proton donor concentration could remarkably suppress the competing HER process. Also, Han and co-workers assembled a hybrid electrolyte system utilizing pure water and 2-propanol.[128] It should be pointed out that the 2-propanol solvent can also improve the N_2 solubility. As a result, the NRR FE of porous Ni catalyst was much higher in 2-propanol and water (v:v, 9:1) mixed electrolyte (0.89%) than that in individual pure water (0.07%). Very recently, Ling et al. developed a hybrid electrolyte including ~1% ethanol in liquid THF and acquired a higher conversion efficiency of N_2-to-NH_3 over the Ag-Au catalyst.[85] Notably, some of the hybrid electrolytes typically composed of THF (solvent) and alcohols (proton source) are also extensively adopted in the Li^+-mediated electrochemical NRR process.[129] Due to the unique non-aqueous environment, the Li^+ within the hybrid electrolytes can be reduced to Li metal, which can spontaneously react with N_2 molecule to form Li_3N at ambient conditions. Subsequently, the Li_3N further reacts with the proton source to generate NH_3. Although a high FE of NH_3 is easily achieved in this route, the poor understanding for the reaction mechanism and the composition of solid electrolyte interphase is still the main reason that limits its development.[80] Besides, the ILs can be also employed as the solvent of hybrid electrolyte to limit the concentration of proton donor. For example, MacFarlane and co-workers used a hybrid electrolyte containing trace amounts of water (~100 ppm) by utilizing $[P_{6,6,6,14}][eFAP]$ as a solvent.[130] Benefiting from the high N_2 solubility of IL-based electrolyte and the effectively inhibited H_2 evolution induced by the controllable water content, a high NRR FE of 60% for Fe-based catalyst was achieved in this hybrid electrolyte. In order to regulate the proton donor (H_2O) concentration more precisely, the authors further developed a mixed solvent system of $[C_4mpyr][eFAP]$ ILs and aprotic 1H,1H,5H-octafluoropentyl-1,1,2,2-tetrafluoroethyl ether (FPEE).[131] In virtue of the well-designed mixed solvent, the water content was precisely controlled in a range of 1–200 ppm, and correspondingly, the HER activity could be manipulated effectively. The optimal water content of the mixed solvent was confirmed to be 120 ppm for a β-FeOOH nanorod catalyst, eventually achieving a NRR FE of 32%. Taken together, using aprotogenic or low-proton solvents can efficiently regulate the proton donor concentration, thereby impeding the HER activity and boosting the NRR selectivity. In this connection, the "water-in-salt" electrolyte with adjustable free water content can effectively restrict the water splitting process and deserves exploration in NRR field.[132-134]

5. Catalyst design for retarding the HER activity

In general, the H atoms are much easier to be adsorbed on the surfaces of catalysts in contrast to N_2 molecules, thereby occupying most active sites and consuming the majority of available electrons, eventually leading to a fast yet an undesirable H_2 evolution and a rather low NRR selectivity.[70,135,136] According to this point, the present strategies for suppressing HER activity of NRR electrocatalysts usually involve in mitigating the adsorption towards H atom. To be more specific, they can be grouped into two aspects as follows: 1) designing of catalysts with intrinsic HER restriction such as early transition metal-based (Ti, Zr, Y, and Sc) and atomically dispersed catalysts; 2) engineering the catalysts to suppress HER activity by employing the HER-inactive supports, incorporating the HER-inactive species, blocking the active sites for H_2 evolution, adjusting the crystal phase, and introducing strained effects.

5.1. Selecting the catalysts with intrinsic HER restriction

5.1.1. Early transition metal-based catalysts. Nørskov's group theoretically calculated the free energies for the adsorption and reduction processes of N and H atoms on the flat and stepped surfaces of extensive metals in an acidic electrolyte.[137] It could be seen from Fig. 9a that most of metals were more in favor of binding H atoms compared with N atoms (the gray shading), resulting in an unexpected HER process. In nature, the Mo, Fe, Rh, W, and Ru metals were located on the top of volcano plots, indication of the intrinsically high activity for NRR process. Nevertheless, these metals exhibited the higher adsorption ability towards H atom over N atom, which would lead to a low selectivity of NRR. Clearly, only the surfaces of early transition metals including Ti, Zr, Y, and Sc exhibited stronger binding ability towards N atoms than H atoms, indicative of the intrinsic restriction for HER process. In this regard, these metals and corresponding complexes may be the promising candidates for electrochemical NH_3 synthesis. For instance, Wang et al. revealed that the $Ti_3C_2T_x$ MXene nanosheets exhibited high adsorption ability for N_2 molecule in contrast to H_2O molecule.[138] As a result, the $Ti_3C_2T_x$ MXene delivered a NRR FE of 4.62% at a potential of –0.1 V (*vs.* RHE). Likewise, Sun's group fabricated a TiO_2 nanosheet on Ti foil for electrochemical NRR and obtained a FE of 3.34%.[139] Afterwards, the authors also developed a TiO_2 nanowire on Ti mesh for NRR process.[140] In addition, Xian and co-workers revealed that the ZrO_2 nanoparticles presented a NRR FE of ~4%.[141] Li et al. reported a Y_2O_3 nanosheet as an efficient NRR electrocatalyst and attained the highest FE of 2.53% at a relatively negative potential of –0.9 V (*vs.* RHE).[142] Shui's group confirmed that the Sc_2O_3 nanoparticles could also be utilized as the NRR electrocatalysts.[143] Summarily, although the Ti-, Zr-, Y-, and Sc-based catalysts feature poor binding ability for H atoms, their activity for NRR are still unsatisfactory (FE < 5%) due to the poor intrinsic catalytic activity for NRR. Accordingly, enormous studies focused on improving the intrinsic catalytic activity of electrocatalyst for NRR, including heteroatom doping (such as Fe-doped TiO_2, V-doped TiO_2, Zr-doped TiO_2, and C-doped TiO_2, Y-doped ZrO_2, etc.),[40,41,43,47,144] atom vacancies (such as O, N, and S vacancies, etc.),[49,139,145–147] and heterostructure (such as CoS_2/TiO_2) engineerings.[148]

Energy & Environmental Science Accepted Manuscript

Please do not adjust margins

View Article Online
DOI: 10.1039/D0EE03596C

Published on 19 January 2021. Downloaded by Dalian University of Technology on 1/24/2021 11:50:40 AM.

5.1.2. Atomically dispersed catalysts. Recently, the single atom catalysts (SACs) with unsaturated coordination configuration and maximized atom-utilization efficiency evoke wide attentions in electrocatalytic NRR field due to the remarkable suppression for undesirable HER.[78,149–151] Theoretically, Jung et al. calculated the adsorption free energy of H atom on a series of metal surfaces (such as Mo, Nb, V, Ir, and Co, etc.) and SACs containing the same metal atoms ($\Delta G_{surface}$(*H) and ΔG_{SAC}(*H)), the results given in Fig. 9b.[152] For most of metals, their ΔG_{SAC}(*H) values were relatively low in contrast to corresponding $\Delta G_{surface}$(*H) values, indicating that the H atom is more easily adsorbed on the surface of metal instead of SACs. In the meantime, they also revealed that several SACs such as Mo@C_3, La@N_3, Sc@N_4, and V@C_3, etc., presented a higher adsorption free energy for N_2 molecule than that for H atom (Fig. 9c), meaning that these SACs were promising NRR catalysts to achieve a high selectivity and activity. In addition, other SACs such as boron monolayer-supported V atom, N-doped black phosphorus-supported Mo atom, MoSSe nanosheet-supported Mo atom, $Mo_2TiC_2O_2$ MXene-supported Zr atom, and CeO_2-supported Mo/Ru atoms were also theoretically confirmed to be able to effectively inhibit the HER process by deadening the H adsorption.[153–157] Experimentally, the Y and Sc-based SACs that were supported on N-doped carbon delivered a NRR FE of 12.1% and 11.2% at ambient conditions, respectively.[143] Wu et al. prepared a SAC of Ni atoms immobilized on N-doped carbon (Ni_x-N-C) for electrocatalytic NRR and confirmed that the Ni-N_3 sites acted as the active sites.[158] A FE of 21% was achieved by the Ni_x-N-C, being higher than that of the same N-doped carbon-supported Ni clusters. Also, utilizing the similar N-doped carbon as substrate, the Mo- and Ru-based SACs were successfully fabricated for electrochemical NH_3 synthesis and attained a FE of 14.6% and 29.6%, respectively.[15,159] By using of graphitic carbon nitride (g-C_3N_4) as the support, Ma and co-workers constructed a Ru-based SAC and obtained a NRR FE of 8.3% at ambient conditions.[160] In addition to N-coordinated SACs, the O-coordinated Fe-SAC was also developed for electrochemical NH_3 synthesis, and it was discovered that the Fe-(O-C_2)$_4$ coordination structure could effectively activate the N_2 molecules.[161] More recently, Zhang's group reported a novel SAC of protrusion-shaped Fe atoms anchored on MoS_2 nanosheets, gaining a high FE 31.6% for electrochemical NRR.[78] Further studies revealed that the protrusion-shaped Fe atom resulted in a unique electron-rich interfacial polarization field, which accelerated the N_2 molecule splitting by electron donation. The researches above indicate that the SACs can deliver a relatively high selectivity for NRR due to the poor adsorption ability for H atoms. The reasons for the weakened H adsorption and the resultant HER suppression of the SACs can be briefly summarized as geometric and electronic effects afforded by SACs.[67,152,154,162,163] In case of the geometric effects, the H atom adsorption preferentially occurs at the abundant bridge and hollow sites on the surface of bulk metal due to its instability of adsorption state at the top sites. While for SACs, the available adsorption sites are only the top sites, thus the H adsorption process is significantly impeded. As for the electronic effects, different from the surface atoms of bulk metal, the metal atoms of SACs are positively charged because of the strong interaction with the support. Owing to the electrostatic repulsion, the adsorption of H atom is impeded,

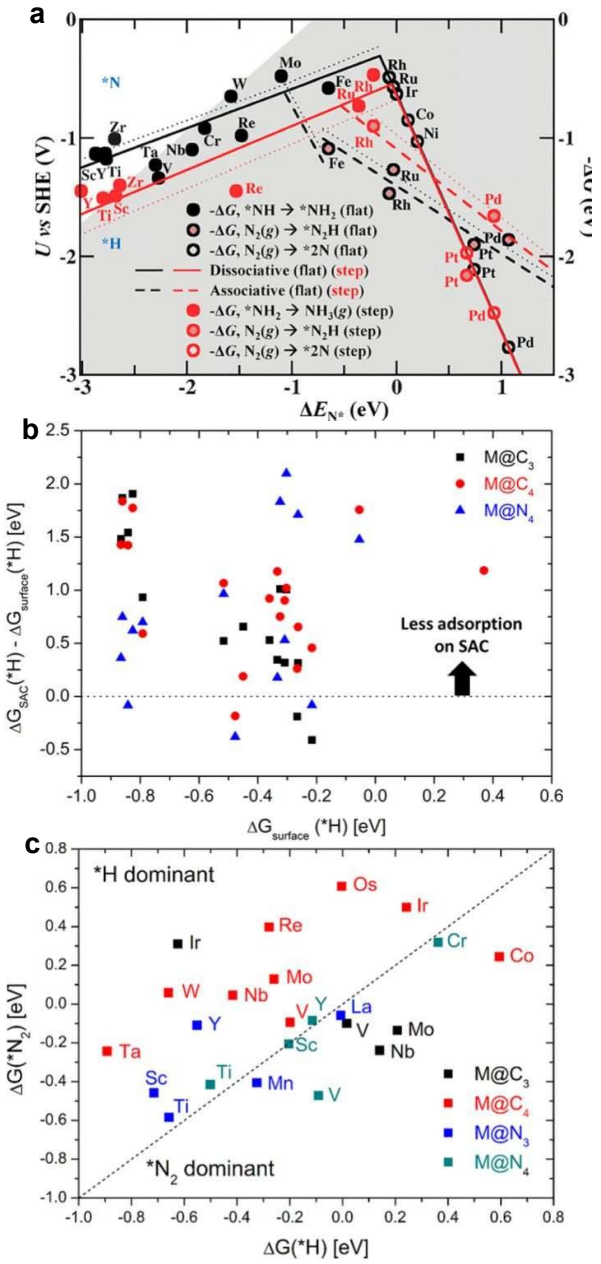

Fig. 9 (a) Combined volcano diagrams (lines) for the flat (black) and stepped (red) transition metal surfaces for N_2 reduction process with a Heyrovsky type reaction, without (solid lines) and with (dotted lines) H-bonding effects. Reproduced with permission from ref.[137]. Copyright 2012, Royal Society of Chemistry. (b) Difference between adsorption free energy of H atom on SACs and the same metal surfaces. (c) The adsorption free energy of SACs for N_2 molecule and H atom. Reproduced with permission from ref.[152]. Copyright 2018, American Chemical Society.

Energy & Environmental Science Accepted Manuscript

This journal is © The Royal Society of Chemistry 20xx

Please do not adjust margins

View Article Online
DOI: 10.1039/D0EE03596C

Published on 19 January 2021. Downloaded by Dalian University of Technology on 1/24/2021 11:50:40 AM.

finally leading to a suppressed HER process. In addition, the double-atom catalysts (DACs) not only feature the merits of the SACs, but also have more tuned active sites and cooperative atomic interactions in contrast to the SACs, receiving increasing attention in electrocatalytic NRR field.[164,165] The homonuclear (such as $Mn_2@C_2N$, $Mo_2@C_2N$, Co_2@graphdiyne, etc.) and heteronuclear DACs (such as TiV@phthalocyanine, VCr@phthalocyanine, etc.) were presented and theoretically confirmed to be much effective for suppressing the undesired HER and achieving a high NRR selectivity.[104,166–168] Besides, a novel N_2 activation mechanism of π-donation/π-backdonation was observed for DACs, which was distinct from the traditional σ-donation/π-backdonation mechanism.[169]

5.2. Engineering the catalysts to suppress HER activity

As mentioned above, it has been confirmed that the H atoms preferentially adsorb on the surfaces of most catalysts compared to N atoms, finally leading to a relatively low NRR selectivity. As such, to achieve a high selectivity, the HER activity of catalysts should be efficiently inhibited via the catalyst engineering. A series of strategies were built such as adopting the supports with poor HER activity, introducing the species with poor HER activity, blocking the HER active sites, regulating the crystal phase, and introducing strained effects (Fig. 10).

As for the supports, previous studies revealed that adopting the materials with poor HER activity (such as FeOOH, FeS_2, MoS_2, and N,P-codoped carbon nanosheets) could mitigate the HER activity of the catalysts.[46,78,138,170] It was noteworthy that the support could not only suppress the H_2 evolution by itself, but also was helpful for the active species to inhibit the HER process due to the strong electronic interactions with the active species. In addition, direct introduction of the species with poor HER activity into catalysts can also impede the undesirable H_2 evolution. For instance, Wang et al. constructed a PdPb nanosponge for electrochemical NRR and confirmed that the presence of Pb could remarkably weaken the adsorption of H atoms, resulting in an inhibited HER process.[171] This is also the case for RuO_2 nanoparticle catalyst. Similarly, incorporating the HER-inactive Y_2O_3 or ZrO_2 nanoparticles into electrocatalysts could also effectively retard the HER process.[45,141] Moreover, the HER activity can also be suppressed by blocking the corresponding HER-active sites of the catalysts. For example, Wang et al. investigated the poly(N-ethyl-benzene-1,2,4,5-tetracarboxylic diimide) (PEBCD) as a NRR electrocatalyst and found that the Li^+ ions could interact with the O atoms (served as active sites for HER) of PEBCD.[172] Owing to the blocking effects, the Tafel or Heyrovsky reaction steps of HER were obviously retarded and a high NRR selectivity was delivered. Likewise, Zhao and co-workers reported that the Li^+ ions were also effective for blocking the S sites (active sites for HER) of MoS_2 nanosheet due to the strong Li–S interactions.[50] As a result, a high NRR FE of 9.81% was achieved by the Li^+-incorporated MoS_2 nanosheets, approximately 18 times more than that of the unmodified MoS_2 (0.53%). Very recently, to mask the HER-active sites (the edge defects) of WS_2 nanosheets, Yang et al. presented a strategy of introducing the HER-inactive WO_2 nanosheet into the edge defects of WS_2 nanosheet.[173] It was discovered that the WO_2-modified WS_2 nanosheets delivered a high NRR FE of 13.5%, superior than that (7.87%) of individual WS_2 nanosheets. In some cases, regulating the crystal phase of catalyst has also been reported to be effective for mitigating the HER process. For instance, MacFarlane et al. revealed that the semiconducting-typed MoS_2 (2H-MoS_2) exhibited a strong suppression for HER in contrast to the metallic type MoS_2 (1T-MoS_2).[174] As a result, the Ru-decorated 2H-MoS_2 catalyst presented a high NRR FE and NH_3 yield rate compared with the Ru-decorated 1T-MoS_2 catalyst. This is also the case for other semiconducting materials (such as CeO_x, BiOCl, etc.).[145,175] Besides, the crystal phase engineering could also boost the intrinsic catalytic activity for N_2 reduction owing to the rationally regulated electronic structure.[176,177] With regard to the strained effects, Zhang et al. recently found that the tensile lattice strains of Ru nanoclusters triggered by O dopants could effectively suppress the HER process.[178] This was because the lattice strains had a crippling effect on the dimerization of H radicals. Meanwhile, the resultant hydrogen radicals accelerated the hydrogenation process of the intermediates for NH_3 synthesis. Additionally, the strained effects were also found to be in favor of activating and dissociating the N_2 molecules.[40] It can be concluded that above strategies for suppressing the HER mainly focus on mitigating the adsorption for H_2O or H_3O^+ as well as inhibiting the dimerization of H radicals. As such, these strategies are effective in full-pH range electrolytes. In another case, there exists the strategy that only works in the acidic electrolytes. On the basis of the Lewis acid property of H_3O^+, the corresponding approach involve in constructing the Lewis acid sites in electrocatalysts, so that the adsorption process of H_3O^+ on electrocatalysts can be effectively inhibited. For instance, Zeng et al. recently developed a F-doped porous carbon with poor HER activity for selectively electrochemical NH_3 synthesis.[179] Due to the difference in electronegativity between F and C atoms, the C atoms bonded with F atoms served as the Lewis acid sites. Therefore, the repulsive interaction between the C atoms and

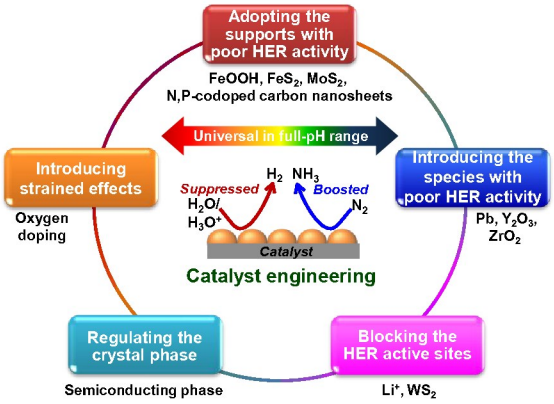

Fig. 10 Strategies for suppressing the HER process via catalyst engineering including adopting the supports with poor HER activity, introducing the species with poor HER activity, blocking the HER active sites, regulating the crystal phase, and introducing strained effects.

Energy & Environmental Science Accepted Manuscript

Please do not adjust margins

View Article Online
DOI: 10.1039/D0EE03596C

Published on 19 January 2021. Downloaded by Dalian University of Technology on 1/24/2021 11:50:40 AM.

H_3O^+ was significantly enhanced, finally resulting in a suppressed adsorption towards H_3O^+ and poor HER activity.

In addition to enhancing the adsorption of N_2 molecule as discussed above, promoting the adsorption of N_xH_y intermediates over the surface of electrocatalyst is also crucial for suppressing HER. However, the corresponding approaches are relatively limited and mainly focus on the modification for the electrolytes at present. Quite recently, Lopez et al. adopted a IL of $[C_4C_1pyrr][FAP]$ to boost the adsorption and stabilization of N_xH_y intermediates and increase the selectivity of NRR.[180] It was found that the competitive adsorption between H atom of water and N_xH_y intermediates can be well regulated in this IL-based environment. Using the density functional theory calculation, they revealed that the N_xH_y intermediates can be effectively adsorbed and stabilized on the surface of Ru-based catalyst due to the H-bonding interactions between N_xH_y and $[FAP]^-$ anions. Meanwhile, the adsorption of H atoms was greatly inhibited, finally leading to the suppressed HER activity. Similarly, Nørskov and co-workers chose non-aqueous 2,6-lutidinium ($LutH^+$) as the proton donor for electrochemical NRR and confirmed that the $LutH^+$ can also selectively stabilize the N_xH_y intermediates rather than the adsorbed H atoms via formation of H-bonding.[181] As a result, the adsorption process of H atoms on Pt(111) was efficiently mitigated, and the corresponding H_2 evolution process was also significantly prohibited. Besides, adjusting the electronic structure or surface property of NRR electrocatalyst may also be an effective method to change the binding energy of N_xH_y intermediates and H atoms, which should be paid more attention to in future.

6. Conclusions and perspectives

In conclusion, the strategies for suppressing the competing H_2 evolution to boost the electrochemical NRR selectivity have been presented from the perspective of reaction kinetics and thermodynamics as well as catalyst engineering. On the basis of the mechanism of NRR, limiting the accessibility of proton from the electrolyte and electron over the surface of catalyst derived from the external circuit can effectively inhibit the kinetically preferred HER, eventually leading to an enhanced NRR selectivity. It is noteworthy that excessively restricting on the accessibility of proton and electron may hinder the whole conversion efficiency of NRR to some degree, thus the balance between selectivity and conversion efficiency should be taken into consideration when taking the corresponding strategies. The scenario for shifting the reaction equilibrium of HER can efficiently impede the notorious HER in this process and boost the NRR selectivity; meanwhile, the corresponding energy consumption needs to be considered. The approaches to catalyst engineering for optimizing and mitigating the adsorption of H species are presented, which can directly retard the H_2 evolution. Of course, this design philosophy/concept for catalyst is under the premise of the apparent and intrinsic catalytic activities for NRR. These strategies for HER suppression can be utilized in combination. In spite of these significant progresses, the selectivity and efficiency for NRR still need to be improved for promoting the practical application, and the following aspects need to be considered (Fig. 11).

i) Building rigorous protocols for precise NH_3 determination

Currently, the amount of produced NH_3 by electrochemical NRR process is relatively low and keeps at the microgram level.[182] Furthermore, the possible NH_3 contamination is commonly present in atmosphere, ion exchange membranes, and even the electrocatalyst itself.[8,23,183,184] Accordingly, it is quiet challenging for precise determination of the produced NH_3. Recently, the rigorous protocols for precise and reliable NH_3 determination have been constructed by researchers, where a series of the controlled experiments should be carried out in the following conditions such as under Ar gas atmosphere, at open-circuit potential, in the absence of electrocatalysts, and under $^{15}N_2$ gas atmosphere, to exclude the possible ammonia contamination.[22] Especially for the system with the NH_3 yield rate less than 10 nmol s^{-1} cm^{-2}, the quantitative $^{15}N_2$ tests are highly required in order to make the results more reliable.[185] In addition, except for the FE, we also call the NRR community to use the partial current density of NH_3 and the NH_3 yield rates normalized both by mass of electrocatalyst and geometric area of electrode as the descriptors for NRR performance. Only with these reliable data, we can well evaluate and design the high-efficiency electrocatalysts, and fast facilitate the development of electrocatalytic NRR in future.

ii) Optimizing electrocatalysts to enhance the activation ability towards N_2

Great progress for boosting the activation ability of electrocatalysts towards N_2 has been made up to now, with the focus of defects, heterostructure, strains, and crystallinity engineering, etc.[186,187] However, the activation ability of electrocatalysts towards N_2 is still insufficient, which also serves as an elementary roadblock for high-efficiency ammonia synthesis under ambient conditions due to the high activation barrier of N_2 molecule. In fact, in organometallic/inorganometallic chemistry fields, it has been proved that the Gadolinium (Gd), Tantalum (Ta), and Samarium (Sm) metal centers feature enough electron density to weaken and cleave the N≡N bond under mild conditions.[127,188,189] Besides, in traditional Haber–Bosch process, it has been demonstrated that the basic promoters (K_2O, Na_2O, BaO_x, $Cs_{2-x}O$ and so on) and electrides (for example, $Ca_{24}Al_{28}O_{64}^{4+}(e^-)_4$ and $Y_5Si_3^{0.79+}(e^-)_{0.79}$) can also donate electrons to the antibonding π-orbitals of N_2 molecule and then facilitate the activation process for N_2 molecule.[56,190,191] Nevertheless, these strategies to promote the N_2 cleavage are rarely reported in electrochemical NRR field. Alternatively, these may be helpful to develop the novel electrocatalysts for effectively electrochemical NH_3 synthesis in future, with a major challenge.

iii) Regulating the gas-liquid-solid three-phase interface

Energy & Environmental Science Accepted Manuscript

This journal is © The Royal Society of Chemistry 20xx

Please do not adjust margins

View Article Online
DOI: 10.1039/D0EE03596C

Published on 19 January 2021. Downloaded by Dalian University of Technology on 1/24/2021 11:50:40 AM.

The electrocatalytic N_2 reduction involves the gas (N_2), liquid (electrolyte), and solid (catalyst) three phases. A series of processes including the diffusion and adsorption of N_2 molecule, the delivery of protons and electrons, as well as the desorption of N_xH_y intermediates and NH_3 molecule, take place simultaneously at the three-phase interface. Previous studies revealed that the local concentration of N_2 molecules and protons near the catalyst surface could remarkably affect the adsorption process of N_2 and protons, respectively. As such, more efforts should also be devoted to the interface engineering covering electrolyte and electrocatalyst. In particular, for the electrolytes, the kinds of proton donors and solvents as well as the additives such as alkali metal ions play significant part in reducing the activity of HER and enhancing the selectivity of NRR. As for the electrocatalysts, regulating its surface property such as hydrophilicity/hydrophobicity can also effectively control the accessibility of proton donors and the local pH value at the interface, thereby greatly inhibiting the competing H_2 evolution. It is expected that the well-regulated three-phase interface can boost the NRR selectivity and activity. Nevertheless, there is still a striking lack of comprehensive and in-depth investigation for the three-phase interface by using of the advanced characterization techniques such as *in situ* X-ray absorption spectroscopy (XAS), *in situ* surface-enhanced infrared absorption spectroscopy (SEIRAS), and *in situ* surface-enhanced Raman spectroscopy (SERS), etc.

iv) Coupling NRR with oxidation reactions to make value-added chemicals

In general, the cathodic NRR occurs jointly with the anodic oxygen evolution reaction (OER). Due to the sluggish OER kinetics, the overall electrolysis voltage is very high and the electrolysis rate is also restricted.[192] Furthermore, the value of anodic oxidation product (O_2) is relatively low. To address these issues, the OER needs to be replaced by the value-added oxidation reactions for the synthesis of fine chemicals in NRR process. Unfortunately, to the best of our knowledge, the reports of the coupling systems are quite limited in NRR field. Alternatively, the electrochemical NRR process can be coupled with the electrooxidation of small molecules that has been well developed in water splitting, for example, glycerol, alcohols, urea, formic acid, 5-hydroxymethylfurfural (HMF), etc., which provides new opportunity for simultaneous synthesis of NH_3 and value-added products.[192–194] Furthermore, this coupling strategy can also effectively improve the energy efficiency of electrochemical NH_3 synthesis process, and may promote the selectivity and activity of NRR to some degree.

v) Developing the flow cell reactor

At present, the electrochemical NRR are mainly carried out in the H-type cells, in which the catalyst is fully inserted into the aqueous electrolyte and the N_2 molecule is dissolved in the electrolyte and diffuses to the catalyst surface via the electrolyte. Because of low solubility of N_2 in aqueous electrolyte, the mass transfer of N_2 is severely limited, which also leads to the restriction of NRR selectivity and efficiency. In contrast, the flow cell reactor equipped with gas-diffusion electrode (GDE) can effectively alleviate the limitation of low N_2 solubility within electrolyte, in which the GDE is typically

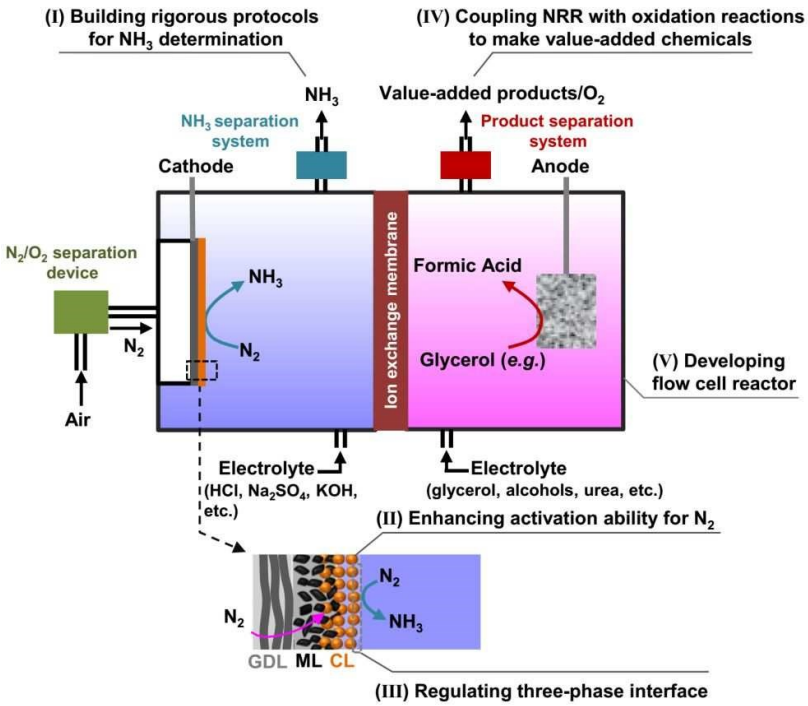

Fig. 11 Perspectives for improving the selectivity and efficiency of electrochemical NRR for promising practical applications. The GDL, MPL, and CL are the abbreviations for the gas-diffusion layer, microporous layer, and catalyst layer, respectively.

Energy & Environmental Science Accepted Manuscript

Please do not adjust margins

View Article Online
DOI: 10.1039/D0EE03596C

Published on 19 January 2021. Downloaded by Dalian University of Technology on 1/24/2021 11:50:40 AM.

composed of gas-diffusion layer (GDL), microporous layer (ML), and catalyst layer (CL) (see Fig. 11). Meanwhile, the flow cell can also quickly remove the produced NH_3 from the surface of electrocatalyst. However, the corresponding investigations are quite limited in NRR field. In other words, integrating the commercial N_2/O_2 separation device/system, value-added oxidation reaction, and efficient separation systems for NH_3 and the value-added products into flow cell reactor may be a promising way to achieve the practical applications for electrochemical NH_3 production in future, with a major challenge in future.

Acknowledgements

This work was partly supported by the National Natural Science Foundation of China (NSFC, Nos. 51872035 and 22078052), Talent Program of Rejuvenation of the Liaoning (No. XLYC1807002), the Fundamental Research Funds for the Central Universities (DUT19LAB20) and the National Key Research Development Program of China (2016YFB0101201).

Conflicts of interest

There are no conflicts to declare.

References

1. J. G. Chen, R. M. Crooks, L. C. Seefeldt, K. L. Bren, R. M. Bullock, M. Y. Darensbourg, P. L. Holland, B. Hoffman, M. J. Janik, A. K. Jones, M. G. Kanatzidis, P. King, K. M. Lancaster, S. V. Lymar, P. Pfromm, W. F. Schneider and R. R. Schrock, *Science*, 2018, **360**, eaar6611.
2. J. W. Erisman, M. A. Sutton, J. Galloway, Z. Klimont and W. Winiwarter, *Nat. Geosci.*, 2008, **1**, 636–639.
3. R. F. Service, *Science*, 2014, **345**, 610.
4. W. Guo, K. Zhang, Z. Liang, R. Zou and Q. Xu, *Chem. Soc. Rev.*, 2019, **48**, 5658–5716.
5. A. J. Martín, T. Shinagawa and J. Pérez-Ramírez, *Chem*, 2018, **5**, 263–283.
6. A. J. Medford and M. C. Hatzell, *ACS Catal.*, 2017, **7**, 2624–2643.
7. G. Marnellos and M. Stoukides, *Science*, 1998, **282**, 98–100.
8. C. Tang and S.-Z. Qiao, *Chem. Soc. Rev.*, 2019, **48**, 3166–3180.
9. M. Li, H. Huang, J. Low, C. Gao, R. Long and Y. Xiong, *Small Methods*, 2018, **3**, 1800388.
10. G.-F. Chen, S. Ren, L. Zhang, H. Cheng, Y. Luo, K. Zhu, L.-X. Ding and H. Wang, *Small Methods*, 2018, **3**, 1800337.
11. E. E. van Tamelen and D. A. Seeley, *J. Am. Chem. Soc.*, 1969, **91**, 5194–5194.
12. V. Kordali, G. Kyriacou and C. Lambrou, *Chem. Commun.*, 2000, 1673–1674.
13. J. Han, X. Ji, X. Ren, G. Cui, L. Li, F. Xie, H. Wang, B. Li and X. Sun, *J. Mater. Chem. A*, 2018, **6**, 12974–12977.
14. H. Cheng, L. X. Ding, G. F. Chen, L. Zhang, J. Xue and H. Wang, *Adv. Mater.*, 2018, **30**, 1803694.
15. Z. Geng, Y. Liu, X. Kong, P. Li, K. Li, Z. Liu, J. Du, M. Shu, R. Si and J. Zeng, *Adv. Mater.*, 2018, **30**, 1803498.
16. W. Guo, Z. Liang, J. Zhao, B. Zhu, K. Cai, R. Zou and Q. Xu, *Small Methods*, 2018, **2**, 1800204.
17. L. Hu, A. Khaniya, J. Wang, G. Chen, W. E. Kaden and X. Feng, *ACS Catal.*, 2018, **8**, 9312–9319.
18. L. Zhang, L. X. Ding, G. F. Chen, X. Yang and H. Wang, *Angew. Chem. Int. Ed.*, 2018, **58**, 2612–2616.
19. M. Nazemi and M. A. El-Sayed, *J. Phys. Chem. Lett.*, 2018, **9**, 5160–5166.
20. J. Wang, L. Yu, L. Hu, G. Chen, H. Xin and X. Feng, *Nat. Commun.*, 2018, **9**, 1795.
21. Y. Wang, X. Cui, J. Zhao, G. Jia, L. Gu, Q. Zhang, L. Meng, Z. Shi, L. Zheng, C. Wang, Z. Zhang and W. Zheng, *ACS Catal.*, 2018, **9**, 336–344.
22. S. Z. Andersen, V. Čolić, S. Yang, J. A. Schwalbe, A. C. Nielander, J. M. McEnaney, K. Enemark-Rasmussen, J. G. Baker, A. R. Singh, B. A. Rohr, M. J. Statt, S. J. Blair, S. Mezzavilla, J. Kibsgaard, P. C. K. Vesborg, M. Cargnello, S. F. Bent, T. F. Jaramillo, I. E. L. Stephens, J. K. Nørskov and I. Chorkendorff, *Nature*, 2019, **570**, 504–508.
23. J. Kibsgaard, J. K. Nørskov and I. Chorkendorff, *ACS Energy Lett.*, 2019, **4**, 2986–2988.
24. G. Qing, R. Ghazfar, S. T. Jackowski, F. Habibzadeh, M. M. Ashtiani, C. P. Chen, M. R. Smith and T. W. Hamann, *Chem. Rev.*, 2020, **120**, 5437–5516.
25. H. Xu, K. Ithisuphalap, Y. Li, S. Mukherjee, J. Lattimer, G. Soloveichik and G. Wu, *Nano Energy*, 2020, **69**, 104469.
26. D. R. MacFarlane, P. V. Cherepanov, J. Choi, B. H. R. Suryanto, R. Y. Hodgetts, J. M. Bakker, F. M. Ferrero Vallana and A. N. Simonov, *Joule*, 2020, **4**, 1186–1205.
27. J. Wang, B. Huang, Y. Ji, M. Sun, T. Wu, R. Yin, X. Zhu, Y. Li, Q. Shao and X. Huang, *Adv. Mater.*, 2020, **32**, 1907112.
28. E. E. van Tamelen, D. A. Seeley, S. W. Schneller, H. Rudler and W. Cretney, *J. Am. Chem. Soc.*, 1970, **92**, 5251–5253.
29. A. Sclafani, V. Augugliaro and M. Schiavello, *J. Electrochem. Soc.*, 1983, **130**, 734–736.
30. J. Y. Becker, S. Avraham and B. Posin, *J. Electroanal. Chem. Interfacial Electrochem.*, 1987, **230**, 143–153.
31. N. Furuya and H. Yoshiba, *J. Electroanal. Chem. Interfacial Electrochem.*, 1989, **263**, 171–174.
32. N. Furuya and H. Yoshiba, *J. Electrochem. Soc.*, 1990, **291**, 269–272.
33. R. Lan, J. T. Irvine and S. Tao, *Sci. Rep.*, 2013, **3**, 1145.
34. X. Li, T. Li, Y. Ma, Q. Wei, W. Qiu, H. Guo, X. Shi, P. Zhang, A. M. Asiri, L. Chen, B. Tang and X. Sun, *Adv. Energy Mater.*, 2018, **8**, 1801357.
35. D. Bao, Q. Zhang, F.-L. Meng, H.-X. Zhong, M.-M. Shi, Y. Zhang, J.-M. Yan, Q. Jiang and X.-B. Zhang, *Adv. Mater.*, 2017, **29**, 1604799.
36. X. Yang, J. Nash, J. Anibal, M. Dunwell, S. Kattel, E. Stavitski, K. Attenkofer, J. G. Chen, Y. Yan and B. Xu, *J. Am. Chem. Soc.*, 2018, **140**, 13387–13391.
37. M.-M. Shi, D. Bao, B.-R. Wulan, Y.-H. Li, Y.-F. Zhang, J.-M. Yan and Q. Jiang, *Adv. Mater.*, 2017, **29**, 1606550.
38. X. Yu, P. Han, Z. Wei, L. Huang, Z. Gu, S. Peng, J. Ma and G. Zheng, *Joule*, 2018, **2**, 1610–1622.
39. C.-C. Chang, S.-R. Li, H.-L. Chou, Y.-C. Lee, S. Patil, Y.-S. Lin, C.-C. Chang, Y. J. Chang and D.-Y. Wang, *Small*, 2019, **15**, 1904723.
40. N. Cao, Z. Chen, K. Zang, J. Xu, J. Zhong, J. Luo, X. Xu and G. Zheng, *Nat. Commun.*, 2019, **10**, 2877.
41. Q. Qin, Y. Zhao, M. Schmallegger, T. Heil, J. Schmidt, R. Walczak, G. Gescheidt-Demner, H. Jiao and M. Oschatz,

Energy & Environmental Science Accepted Manuscript

This journal is © The Royal Society of Chemistry 20xx

Please do not adjust margins

View Article Online
DOI: 10.1039/D0EE03596C

Published on 19 January 2021. Downloaded by Dalian University of Technology on 1/24/2021 11:50:40 AM.

Angew. Chem. Int. Ed., 2019, **58**, 13101–13106.
42. J. Zheng, Y. Lyu, M. Qiao, J. P. Veder, R. D. Marco, J. Bradley, R. Wang, Y. Li, A. Huang, S. P. Jiang and S. Wang, *Angew. Chem. Int. Ed.*, 2019, **58**, 18604–18609.
43. T. Wu, Z. Xing, S. Mou, C. Li, Y. Qiao, Q. Liu, X. Zhu, Y. Luo, X. Shi, Y. Zhang and X. Sun, *Angew. Chem. Int. Ed.*, 2019, **58**, 18449–18453.
44. J. Chen, H. Wang, Z. Wang, S. Mao, J. Yu, Y. Wang and Y. Wang, *ACS Catal.*, 2019, **9**, 5302–5307.
45. H. Tao, C. Choi, L.-X. Ding, Z. Jiang, Z. Han, M. Jia, Q. Fan, Y. Gao, H. Wang, A. W. Robertson, S. Hong, Y. Jung, S. Liu and Z. Sun, *Chem*, 2019, **5**, 204–214.
46. M. Yuan, H. Zhang, D. Gao, H. He, Y. Sun, P. Lu, S. Dilpazir, Q. Li, L. Zhou, S. Li, Z. Liu, J. Yang, Y. Xie, H. Zhao and G. Zhang, *J. Mater. Chem. A*, 2020, **8**, 2691–2700.
47. T. Wu, W. Kong, Y. Zhang, Z. Xing, J. Zhao, T. Wang, X. Shi, Y. Luo and X. Sun, *Small Methods*, 2019, **3**, 1900356.
48. J. Feng, X. Zhu, Q. Chen, W. Xiong, X. Cheng, Y. Luo, A. A. Alshehri, K. A. Alzahrani, Z. Jiang and W. Li, *J. Mater. Chem. A*, 2019, **7**, 26227–26230.
49. H. Jin, L. Li, X. Liu, C. Tang, W. Xu, S. Chen, L. Song, Y. Zheng and S.-Z. Qiao, *Adv. Mater.*, 2019, **31**, 1902709.
50. Y. Liu, M. Han, Q. Xiong, S. Zhang, C. Zhao, W. Gong, G. Wang, H. Zhang and H. Zhao, *Adv. Energy Mater.*, 2019, **9**, 1803935.
51. F. Xu, L. Zhang, X. Ding, M. Cong, Y. Jin, L. Chen and Y. Gao, *Chem. Commun.*, 2019, **55**, 14111–14114.
52. M. A. Shipman and M. D. Symes, *Catal. Today*, 2017, **286**, 57–68.
53. C. J. van der Ham, M. T. Koper and D. G. Hetterscheid, *Chem. Soc. Rev.*, 2014, **43**, 5183–5191.
54. X. Cui, C. Tang and Q. Zhang, *Adv. Energy Mater.*, 2018, **8**, 1800369.
55. X.-F. Li, Q.-K. Li, J. Cheng, L. Liu, Q. Yan, Y. Wu, X.-H. Zhang, Z.-Y. Wang, Q. Qiu and Y. Luo, *J. Am. Chem. Soc.*, 2016, **138**, 8706–8709.
56. S. L. Foster, S. I. P. Bakovic, R. D. Duda, S. Maheshwari, R. D. Milton, S. D. Minteer, M. J. Janik, J. N. Renner and L. F. Greenlee, *Nat. Catal.*, 2018, **1**, 490–500.
57. X. Chen, Y. Guo, X. Du, Y. Zeng, J. Chu, C. Gong, J. Huang, C. Fan, X. Wang and J. Xiong, *Adv. Energy Mater.*, 2019, **10**, 1903172.
58. Y. Abghoui, A. L. Garden, V. F. Hlynsson, S. Bjorgvinsdottir, H. Olafsdottir and E. Skulason, *Phys. Chem. Chem. Phys.*, 2015, **17**, 4909–4918.
59. Y. Abghoui and E. Skúlason, *Catal. Today*, 2017, **286**, 69–77.
60. Y. Abghoui, A. L. Garden, J. G. Howalt, T. Vegge and E. Skúlason, *ACS Catal.*, 2015, **6**, 635–646.
61. J. John, D. K. Lee and U. Sim, *Nano Converg.*, 2019, **6**, 1–16.
62. C. Guo, J. Ran, A. Vasileff and S.-Z. Qiao, *Energy Environ. Sci.*, 2018, **11**, 45–56.
63. S. Wang, F. Ichihara, H. Pang, H. Chen and J. Ye, *Adv. Funct. Mater.*, 2018, **28**, 1803309.
64. Y. Huang, D. D. Babu, Z. Peng and Y. Wang, *Adv. Sci.*, 2020, **7**, 1902390.
65. J. Deng, J. A. Iñiguez and C. Liu, *Joule*, 2018, **2**, 846–856.
66. A. R. Singh, B. A. Rohr, J. A. Schwalbe, M. Cargnello, K. Chan, T. F. Jaramillo, I. Chorkendorff and J. K. Nørskov, *ACS Catal.*, 2016, **7**, 706–709.
67. Z. W. Seh, J. Kibsgaard, C. F. Dickens, I. Chorkendorff, J. K. Nørskov and T. F. Jaramillo, *Science*, 2017, **355**, eaad4998.
68. D. V. Yandulov and R. R. Schrock, *Science*, 2003, **301**, 76–78.
69. M. Dunwell, Y. Yan and B. Xu, *Curr. Opin. Chem. Eng.*, 2018, **20**, 151–158.
70. L. Hu, Z. Xing and X. Feng, *ACS Energy Lett.*, 2020, **5**, 430–436.
71. K. Yang, R. Kas and W. A. Smith, *J. Am. Chem. Soc.*, 2019, **141**, 15891–15900.
72. A. Goyal, G. Marcandalli, V. A. Mints and M. T. M. Koper, *J. Am. Chem. Soc.*, 2020, **142**, 4154–4161.
73. Y. Mukouyama, R. Nakazato, T. Shiono, S. Nakanishi and H. Okamoto, *J. Electroanal. Chem. (Lausanne)*, 2014, **713**, 39–46.
74. Y. Song, D. Johnson, R. Peng, D. K. Hensley, P. V. Bonnesen, L. Liang, J. Huang, F. Yang, F. Zhang, R. Qiao, A. P. Baddorf, T. J. Tschaplinski, N. L. Engle, M. C. Hatzell, Z. Wu, D. A. Cullen, H. M. Meyer III, B. G. Sumpter and A. J. Rondinone, *Sci. Adv.*, 2018, **4**, 1700336.
75. Y.-C. Hao, Y. Guo, L.-W. Chen, M. Shu, X.-Y. Wang, T.-A. Bu, W.-Y. Gao, N. Zhang, X. Su, X. Feng, J.-W. Zhou, B. Wang, C.-W. Hu, A.-X. Yin, R. Si, Y.-W. Zhang and C.-H. Yan, *Nat. Catal.*, 2019, **2**, 448–456.
76. Q. Zhang, B. Liu, L. Yu, Y. Bei and B. Tang, *ChemCatChem*, 2020, **12**, 334–341.
77. A. Yin, T.-A. Bu, Y. Hao, W.-Y. Gao, X. Su, L.-W. Chen and N. Zhang, *Nanoscale*, 2019, **11**, 10072–10079.
78. J. Li, S. Chen, F. Quan, G. Zhan, F. Jia, Z. Ai and L. Zhang, *Chem*, 2020, **6**, 885–901.
79. N. Lazouski, Z. J. Schiffer, K. Williams and K. Manthiram, *Joule*, 2019, **3**, 1127–1139.
80. S. Z. Andersen, M. J. Statt, V. J. Bukas, S. G. Shapel, J. B. Pedersen, K. Krempl, M. Saccoccio, D. Chakraborty, J. Kibsgaard, P. C. K. Vesborg, J. Nørskov and I. Chorkendorff, *Energy Environ. Sci.*, 2020, **13**, 4291–4300.
81. L. Li, C. Tang, D. Yao, Y. Zheng and S.-Z. Qiao, *ACS Energy Lett.*, 2019, **4**, 2111–2116.
82. B. L. Sheets and G. G. Botte, *Chem. Commun.*, 2018, **54**, 4250–4253.
83. H. Y. F. Sim, J. R. T. Chen, C. S. L. Koh, H. K. Lee, X. Han, G. C. Phan-Quang, J. Y. Pang, C. L. Lay, S. Pedireddy, I. Y. Phang, E. K. L. Yeow and X. Y. Ling, *Angew. Chem. Int. Ed.*, 2020, **59**, 16997–17003.
84. Y. Yang, S. Q. Wang, H. Wen, T. Ye, J. Chen, C. P. Li and M. Du, *Angew. Chem. Int. Ed.*, 2019, **58**, 15362–15366.
85. H. K. Lee, C. S. K. Lin, Y. H. Lee, C. Liu, I. Y. Phang, X. Han, C. Tsung and X. Y. Ling, *Sci. Adv.*, 2018, **4**, eaar3208.
86. C. S. L. Koh, H. K. Lee, H. Y. Fan Sim, X. Han, G. C. Phan-Quang and X. Y. Ling, *Chem. Mater.*, 2020, **32**, 1674–1683.
87. J. Zheng, Y. Lyu, M. Qiao, R. Wang, Y. Zhou, H. Li, C. Chen, Y. Li, H. Zhou, S. P. Jiang and S. Wang, *Chem*, 2019, **5**, 617–633.
88. F. Lai, W. Zong, G. He, Y. Xu, H. Huang, B. Weng, D. Rao, J. A. Martens, J. Hofkens, T. Liu and I. P. Parkin, *Angew. Chem. Int. Ed.*, 2020, **59**, 13320–13327.
89. S. Malkhandi, B. Yang, A. K. Manohar, G. K. Prakash and S. R. Narayanan, *J. Am. Chem. Soc.*, 2013, **135**, 347–353.
90. E. C. Tse, C. J. Barile, N. A. Kirchschlager, Y. Li, J. P. Gewargis, S. C. Zimmerman, A. Hosseini and A. A. Gewirth, *Nat. Mater.*, 2016, **15**, 754–759.
91. D. Tan, C. Cui, J. Shi, Z. Luo, B. Zhang, X. Tan, B. Han, L. Zheng, J. Zhang and J. Zhang, *Nano Res.*, 2019, **12**, 1167–1172.
92. J. Xie, X. Zhao, M. Wu, Q. Li, Y. Wang and J. Yao, *Angew.*

Energy & Environmental Science Accepted Manuscript

Please do not adjust margins

View Article Online
DOI: 10.1039/D0EE03596C

Published on 19 January 2021. Downloaded by Dalian University of Technology on 1/24/2021 11:50:40 AM.

Chem. Int. Ed., 2018, **57**, 9640–9644.
93. H. Li, J. Shang, Z. Ai and L. Zhang, *J. Am. Chem. Soc.*, 2015, **137**, 6393–6399.
94. H. Li, J. Li, Z. Ai, F. Jia and L. Zhang, *Angew. Chem. Int. Ed.*, 2018, **57**, 122–138.
95. P. Wang, Y. Ji, Q. Shao, Y. Li and X. Huang, *Sci. Bull.*, 2020, **65**, 350–358.
96. Y. P. Liu, Y. B. Li, H. Zhang and K. Chu, *Inorg. Chem.*, 2019, **58**, 10424–10431.
97. L. Li, C. Tang, B. Xia, H. Jin, Y. Zheng and S.-Z. Qiao, *ACS Catal.*, 2019, **9**, 2902–2908.
98. P. Li, W. Fu, P. Zhuang, Y. Cao, C. Tang, A. B. Watson, P. Dong, J. Shen and M. Ye, *Small*, 2019, **15**, 1902535.
99. L. Di, X. Chen, Y. T. Liu, J. Yu and B. Ding, *Chem. Commun.*, 2019, **55**, 13892–13895.
100. X. Chen, Y.-T. Liu, C. Ma, J. Yu and B. Ding, *J. Mater. Chem. A*, 2019, **7**, 22235–22241.
101. K. Chu, Y. P. Liu, Y. B. Li, J. Wang and H. Zhang, *ACS Appl. Mater. Interfaces*, 2019, **11**, 31806–31815.
102. L. Zhang, X. Ren, Y. Luo, X. Shi, A. M. Asiri, T. Li and X. Sun, *Chem. Commun.*, 2018, **54**, 12966–12969.
103. Y. Wang, M. M. Shi, D. Bao, F. L. Meng, Q. Zhang, Y. T. Zhou, K. H. Liu, Y. Zhang, J. Z. Wang, Z. W. Chen, D. P. Liu, Z. Jiang, M. Luo, L. Gu, Q. H. Zhang, X. Z. Cao, Y. Yao, M. H. Shao, Y. Zhang, X. B. Zhang, J. G. Chen, J. M. Yan and Q. Jiang, *Angew. Chem. Int. Ed.*, 2019, **58**, 9464–9469.
104. X. Guo, J. Gu, S. Lin, S. Zhang, Z. Chen and S. Huang, *J. Am. Chem. Soc.*, 2020, **142** 5709–5721.
105. F. Köleli, Röpke, D., Aydin, R., Röpke, T., *J. Appl. Electrochem.*, 2011, **41**, 405–413.
106. J. Yu, J. Li, X. Zhu, X. Zhang, K. Jia, W. Kong, P. Wei, H. Chen, X. Shi, A. M. Asiri, Q. Li and X. Sun, *ChemElectroChem*, 2019, **6**, 2215–2218.
107. Y.-X. Lin, S.-N. Zhang, Z.-H. Xue, J.-J. Zhang, H. Su, T.-J. Zhao, G.-Y. Zhai, X.-H. Li, M. Antonietti and J.-S. Chen, *Nat. Commun.*, 2019, **10**, 4380.
108. Y. Tian, M. Liu, X. Zhou, L. Huang, Z. Liu and B. An, *J. Electrochem. Soc.*, 2013, **161**, E23–E27.
109. J. Hemmerling, J. Quinn and S. Linic, *Adv. Energy Mater.*, 2020, **10**, 1903354.
110. A. R. Singh, B. A. Rohr, M. J. Statt, J. A. Schwalbe, M. Cargnello and J. K. Nørskov, *ACS Catal.*, 2019, **9**, 8316–8324.
111. H. Cheng, P. Cui, F. Wang, L.-X. Ding and H. Wang, *Angew. Chem. Int. Ed.*, 2019, **58**, 15541–15547.
112. Z. Yan, M. Ji, J. Xia and H. Zhu, *Adv. Energy Mater.*, 2019, **10**, 1902020.
113. S. Chen, S. Perathoner, C. Ampelli, C. Mebrahtu, D. Su and G. Centi, *Angew. Chem. Int. Ed.*, 2017, **56**, 2699–2703.
114. Y. C. Tan, K. B. Lee, H. Song and J. Oh, *Joule*, 2020, **4**, 1104–1120.
115. X. Cui, C. Tang, X. M. Liu, C. Wang, W. Ma and Q. Zhang, *Chem.-Eur. J.*, 2018, **24**, 18494–18501.
116. F. P. García de Arquer, C.-T. Dinh, A. Ozden, J. Wicks, C. McCallum, A. R. Kirmani, D.-H. Nam, C. Gabardo, A. Seifitokaldani, X. Wang, Y. C. Li, F. Li, J. Edwards, L. J. Richter, S. J. Thorpe, D. Sinton and E. H. Sargent, *Science*, 2020, **367**, 661–666.
117. S. Chen, S. Perathoner, C. Ampelli, C. Mebrahtu, D. Su and G. Centi, *ACS Sustain. Chem. Eng.*, 2017, **5**, 7393–7400.
118. J. Kong, A. Lim, C. Yoon, J. H. Jang, H. C. Ham, J. Han, S. Nam, D. Kim, Y.-E. Sung, J. Choi and H. S. Park, *ACS Sustain. Chem. Eng.*, 2017, **5**, 10986–10995.
119. J. C. McGlynn, T. Dankwort, L. Kienle, N. A. G. Bandeira, J. P. Fraser, E. K. Gibson, I. Cascallana-Matias, K. Kamaras, M. D. Symes, H. N. Miras and A. Y. Ganin, *Nat. Commun.*, 2019, **10**, 4916.
120. Z. Fang, D. Fernandez, N. Wang, Z. Bai and G. Yu, *Sci. China Chem.*, 2020, **63**, 155–157.
121. N. Cao and G. Zheng, *Nano Res.*, 2018, **11**, 2992–3008.
122. S. Mukherjee, D. A. Cullen, S. Karakalos, K. Liu, H. Zhang, S. Zhao, H. Xu, K. L. More, G. Wang and G. Wu, *Nano Energy*, 2018, **48**, 217–226.
123. Y. Luo, L. Tang, U. Khan, Q. Yu, H.-M. Cheng, X. Zou and B. Liu, *Nat. Commun.*, 2019, **10**, 269.
124. J. Zhang, T. Wang, P. Liu, S. Liu, R. Dong, X. Zhuang, M. Chen and X. Feng, *Energy Environ. Sci.*, 2016, **9**, 2789–2793.
125. D. Strmcnik, P. P. Lopes, B. Genorio, V. R. Stamenkovic and N. M. Markovic, *Nano Energy*, 2016, **29**, 29–36.
126. K. Kim, C.-Y. Yoo, J.-N. Kim, H. C. Yoon and J.-I. Han, *J. Electrochem. Soc.*, 2016, **163**, F1523–F1526.
127. Y. Ashida, K. Arashiba, K. Nakajima and Y. Nishibayashi, *Nature*, 2019, **568**, 536–540.
128. K. Kim, N. Lee, C.-Y. Yoo, J.-N. Kim, H. C. Yoon and J.-I. Han, *J. Electrochem. Soc.*, 2016, **163**, F610–F612.
129. J.-L. Ma, D. Bao, M.-M. Shi, J.-M. Yan and X.-B. Zhang, *Chem*, 2017, **2**, 525–532.
130. F. Zhou, L. M. Azofra, M. Ali, M. Kar, A. N. Simonov, C. McDonnell-Worth, C. Sun, X. Zhang and D. R. MacFarlane, *Energy Environ. Sci.*, 2017, **10**, 2516–2520.
131. B. H. R. Suryanto, C. S. M. Kang, D. Wang, C. Xiao, F. Zhou, L. M. Azofra, L. Cavallo, X. Zhang and D. R. MacFarlane, *ACS Energy Lett.*, 2018, **3**, 1219–1224.
132. L. Suo, O. Borodin, T. Gao, M. Olguin, J. Ho, X. Fan, C. Luo, C. Wang and K. Xu, *Science*, 2015, **350**, 938–943.
133. Q. Dong, X. Zhang, D. He, C. Lang and D. Wang, *ACS Cent. Sci.*, 2019, **5**, 1461–1467.
134. L. Yang, J. Yu, R. Fu, Y. Xie, C. Yu and J. Qiu, *J. Chem. Ind. Eng. (China)*, 2020, **71**, 2457–2465.
135. Y. Yao, J. Wang, U. B. Shahid, M. Gu, H. Wang, H. Li and M. Shao, *Electrochem. Energ. Rev.*, 2020, **3**, 239–270.
136. Q. Wang, Y. Lei, D. Wang and Y. Li, *Energy Environ. Sci.*, 2019, **12**, 1730–1750.
137. E. Skulason, T. Bligaard, S. Gudmundsdottir, F. Studt, J. Rossmeisl, F. Abild-Pedersen, T. Vegge, H. Jonsson and J. K. Norskov, *Phys. Chem. Chem. Phys.*, 2012, **14**, 1235–1245.
138. Y. Luo, G.-F. Chen, L. Ding, X. Chen, L.-X. Ding and H. Wang, *Joule*, 2019, **3**, 279–289.
139. R. Zhang, X. Ren, X. Shi, F. Xie, B. Zheng, X. Guo and X. Sun, *ACS Appl. Mater. Interfaces*, 2018, **10**, 28251–28255.
140. B. Li, X. Zhu, J. Wang, R. Xing, Q. Liu, X. Shi, Y. Luo, S. Liu, X. Niu and X. Sun, *Chem. Commun.*, 2020, **56**, 1074–1077.
141. H. Xian, Q. Wang, G. Yu, H. Wang, Y. Li, Y. Wang and T. Li, *Appl. Catal. A Gen.*, 2019, **581**, 116–122.
142. X. Li, L. Li, X. Ren, D. Wu, Y. Zhang, H. Ma, X. Sun, B. Du, Q. Wei and B. Li, *Ind. Eng. Chem. Res.*, 2018, **57**, 16622–16627.
143. J. Liu, X. Kong, L. Zheng, X. Guo, X. Liu and J. Shui, *ACS Nano*, 2020, **14**, 1093–1101.
144. S. Luo, X. Li, M. Wang, X. Zhang, W. Gao, S. Su, G. Liu and M. Luo, *J. Mater. Chem. A*, 2020, **8**, 5647–5654.
145. S. Cheng, Y.-J. Gao, Y.-L. Yan, X. Gao, S.-H. Zhang, G.-L. Zhuang, S.-W. Deng, Z.-Z. Wei, X. Zhong and J.-G. Wang, *J. Energy Chem.* 2019, **39**, 144–151.
146. X. Yang, S. Kattel, J. Nash, X. Chang, J. H. Lee, Y. Yan, J. G. Chen and B. Xu, *Angew. Chem. Int. Ed.*, 2019, **131**, 13906–

Energy & Environmental Science Accepted Manuscript

This journal is © The Royal Society of Chemistry 20xx

Please do not adjust margins

View Article Online
DOI: 10.1039/D0EE03596C

Published on 19 January 2021. Downloaded by Dalian University of Technology on 1/24/2021 11:50:40 AM.

13910.
147. Y. Tong, H. Guo, D. Liu, X. Yan, J. Liang, P. Su, S. Zhou, J. Liu, G. Q. M. Lu and S. X. Dou, *Angew. Chem. Int. Ed.*, 2020, **59**, 7356–7361.
148. B. Ding, Y.-T. Liu, X. Chen and J. Yu, *Angew. Chem. Int. Ed.*, 2019, **58**, 18903–18907.
149. C. Liu, Q. Li, J. Zhang, Y. Jin, D. R. MacFarlane and C. Sun, *J. Mater. Chem. A*, 2019, **7**, 4771–4776.
150. Z. Chen, J. Zhao, C. R. Cabrera and Z. Chen, *Small Methods*, 2018, **3**, 1800368.
151. R. Hao, W. Sun, Q. Liu, X. Liu, J. Chen, X. Lv, W. Li, Y. P. Liu and Z. Shen, *Small*, 2020, **16**, 2000015.
152. C. Choi, S. Back, N.-Y. Kim, J. Lim, Y.-H. Kim and Y. Jung, *ACS Catal.*, 2018, **8**, 7517–7525.
153. H.-R. Zhu, Y.-L. Hu, S.-H. Wei and D.-Y. Hua, *J. Phys. Chem. C*, 2019, **123**, 4274–4281.
154. P. Ou, X. Zhou, F. Meng, C. Chen, Y. Chen and J. Song, *Nanoscale*, 2019, **11**, 13600–13611.
155. L. Li, B. Li, Q. Guo and B. Li, *J. Phys. Chem. C*, 2019, **123**, 14501–14507.
156. L. Li, X. Wang, H. Guo, G. Yao, H. Yu, Z. Tian, B. Li and L. Chen, *Small Methods*, 2019, **3**, 1900337.
157. J. Qi, L. Gao, F. Wei, Q. Wan and S. Lin, *ACS Appl. Mater. Interfaces*, 2019, **11**, 47525–47534.
158. S. Mukherjee, X. Yang, W. Shan, W. Samarakoon, S. Karakalos, D. A. Cullen, K. More, M. Wang, Z. Feng, G. Wang and G. Wu, *Small Methods*, 2020, **4**, 1900821.
159. L. Han, X. Liu, J. Chen, R. Lin, H. Liu, F. Lu, S. Bak, Z. Liang, S. Zhao, E. Stavitski, J. Luo, R. R. Adzic and H. L. Xin, *Angew. Chem. Int. Ed.*, 2019, **58**, 2321–2325.
160. B. Yu, H. Li, J. White, S. Donne, J. Yi, S. Xi, Y. Fu, G. Henkelman, H. Yu, Z. Chen and T. Ma, *Adv. Funct. Mater.*, 2019, **30**, 1905665.
161. H. Zhao, S. Zhang, M. Jin, T. Shi, M. Han, Q. Sun, Y. Lin, Z. Ding, L. R. Zheng, G. Wang, Y. Zhang and H. Zhang, *Angew. Chem. Int. Ed.*, 2020, **59**, 13423–13429.
162. J. Guo, J. Huo, Y. Liu, W. Wu, Y. Wang, M. Wu, H. Liu and G. Wang, *Small Methods*, 2019, **3**, 1900159.
163. T. W. van Deelen, C. Hernández Mejía and K. P. de Jong, *Nat. Catal.*, 2019, **2**, 955–970.
164. H. Li, Z. Zhao, Q. Cai, L. Yin and J. Zhao, *J. Mater. Chem. A*, 2020, **8**, 4533–4543.
165. W. Yang, H. Huang, X. Ding, Z. Ding, C. Wu, I. D. Gates and Z. Gao, *Electrochim. Acta*, 2020, **335**, 135667.
166. Z. W. Chen, J.-M. Yan and Q. Jiang, *Small Methods*, 2018, **3**, 1800291.
167. X. Zhang, A. Chen, Z. Zhang and Z. Zhou, *J. Mater. Chem. A*, 2018, **6**, 18599–18604.
168. D. Ma, Z. Zeng, L. Liu, X. Huang and Y. Jia, *J. Phys. Chem. C*, 2019, **123**, 19066–19076.
169. Y. Qian, Y. Liu, Y. Zhao, X. Zhang and G. Yu, *EcoMat*, 2020, **2**, e12014.
170. H.-B. Wang, J.-Q. Wang, R. Zhang, C.-Q. Cheng, K.-W. Qiu, Y.-j. Yang, J. Mao, H. Liu, M. Du, C.-K. Dong and X.-W. Du, *ACS Catal.*, 2020, **10**, 4914–4921.
171. H. Zhao, D. Zhang, Z. Wang, Y. Han, X. Sun, H. Li, X. Wu, Y. Pan, Y. Qin, S. Lin, Z. Xu, J. Lai and L. Wang, *Appl. Catal. B-Environ.*, 2020, **265**, 118481.
172. G.-F. Chen, X. Cao, S. Wu, X. Zeng, L.-X. Ding, M. Zhu and H. Wang, *J. Am. Chem. Soc.*, 2017, **139**, 9771–9774.
173. Y. Ling, F. M. D. Kazim, S. Ma, Q. Zhang, K. Qu, Y. Wang, S. Xiao, W. Cai and Z. Yang, *J. Mater. Chem. A*, 2020, **8**, 12996–13003.
174. B. H. R. Suryanto, D. Wang, L. M. Azofra, M. Harb, L. Cavallo, R. Jalili, D. R. G. Mitchell, M. Chatti and D. R. MacFarlane, *ACS Energy Lett.*, 2019, **4**, 430–435.
175. Y. Shiraishi, M. Hashimoto, K. Chishiro, K. Moriyama, S. Tanaka and T. Hirai, *J. Am. Chem. Soc.*, 2020, **142**, 7574–7583.
176. W. Tong, B. Huang, P. Wang, L. Li, Q. Shao and X. Huang, *Angew. Chem. Int. Ed.*, 2020, **59**, 2649–2653.
177. J. Zhang, L. Liu, X. Li, S. Huang, X. L. Li, Y. Dong, C. Ling, J. Wang, W. Zang, Z. Kou and H. Y. Yang, *Nanoscale*, 2020, **12**, 10964–10971.
178. J. Li, G. Zhan, J. Yang, F. Quan, C. Mao, Y. Liu, B. Wang, F. Lei, L. Li, A. W. M. Chan, L. Xu, Y. Shi, Y. Du, W. Hao, P. K. Wong, J. Wang, S. X. Dou, L. Zhang and J. C. Yu, *J. Am. Chem. Soc.*, 2020, **142**, 7036–7046.
179. Y. Liu, Q. Li, X. Guo, X. Kong, J. Ke, M. Chi, Q. Li, Z. Geng and J. Zeng, *Adv. Mater.*, 2020, **32**, 1907690.
180. M. A. Ortuno, O. Holloczki, B. Kirchner and N. Lopez, *J. Phys. Chem. Lett.*, 2019, **10**, 513–517.
181. L. Zhang, S. Mallikarjun Sharada, A. R. Singh, B. A. Rohr, Y. Su, L. Qiao and J. K. Norskov, *Phys. Chem. Chem. Phys.*, 2018, **20**, 4982–4989.
182. B. H. R. Suryanto, H.-L. Du, D. Wang, J. Chen, A. N. Simonov and D. R. MacFarlane, *Nat. Catal.*, 2019, **2**, 290–296.
183. Y. Ren, C. Yu, X. Tan, X. Han, H. Huang, H. Huang and J. Qiu, *Small Methods*, 2019, **3**, 1900474.
184. B. Hu, M. Hu, L. Seefeldt and T. L. Liu, *ACS Energy Lett.*, 2019, **4**, 1053–1054.
185. J. Choi, B. H. R. Suryanto, D. Wang, H.-L. Du, R. Y. Hodgetts, F. M. Ferrero Vallana, D. R. MacFarlane and A. N. Simonov, *Nat. Commun.*, 2020, **11**, 5546.
186. H. D. Xiaoxi Guo, Fengli Qu, and Jinghong Li, *J. Mater. Chem. A*, 2019, **7**, 3531–3543.
187. S. Zhao, X. Lu, L. Wang, J. Gale and R. Amal, *Adv. Mater.*, 2019, **31**, 1805367.
188. Z.-Y. Li, L.-H. Mou, G.-P. Wei, Y. Ren, M.-Q. Zhang, Q.-Y. Liu and S.-G. He, *Inorg. Chem.*, 2019, **58**, 4701–4705.
189. C. Geng, J. Li, T. Weiske and H. Schwarz, *Proc. Natl. Acad. Sci.*, 2018, **115**, 11680–11687.
190. M. Kitano, S. Kanbara, Y. Inoue, N. Kuganathan, P. V. Sushko, T. Yokoyama, M. Hara and H. Hosono, *Nat. Commun.*, 2015, **6**, 6731.
191. Y. Lu, J. Li, T. Tada, Y. Toda, S. Ueda, T. Yokoyama, M. Kitano and H. Hosono, *J. Am. Chem. Soc.*, 2016, **138**, 3970–3973.
192. D. Zhao, Z. Zhuang, X. Cao, C. Zhang, Q. Peng, C. Chen and Y. Li, *Chem. Soc. Rev.*, 2020, **49**, 2215–2264.
193. X. Han, H. Sheng, C. Yu, T. W. Walker, G. W. Huber, J. Qiu and S. Jin, *ACS Catal.*, 2020, **10**, 6741–6752.
194. B. You, X. Liu, X. Liu and Y. Sun, *ACS Catal.*, 2017, **7**, 4564–4570.

Energy & Environmental Science Accepted Manuscript

Please do not adjust margins